https://doi.org/10.5194/jecats-2026-14
Preprint. Discussion started: 14 August 2026

Towards the implementation of climate-optimized air traffic in Northern Europe: Feasibility and airspace constraints of pre-tactical contrail mitigation

Dennis Piontek[1], Kai Widmaier[1], Simon Kirschler[1], Joël Clément[2], Jacques Edeline[2], Jakob Smretschnig[3], David Antonello[2], Tarmo Pihlak[4,†], Simone Dietmüller[1], Sigrun Matthes[1], Katrin Dahlmann[1], Feijia Yin[3], and Christiane Voigt[1,5]

[1]Deutsches Zentrum für Luft- und Raumfahrt, Institut für Physik der Atmosphäre, Oberpfaffenhofen, Germany
[2]Thales S.A., Toulouse, France
[3]Delft University of Technology, Faculty of Aerospace Engineering, Operations & Environment, Delft, Netherlands
[4]Estonian Air Navigation Services, Tallinn, Estonia
[5]Johannes Gutenberg Universität, Institut für Physik der Atmosphäre, Mainz, Germany
[†]Present address: Integra Consult A/S, Vedbæk, Denmark

Correspondence: Dennis Piontek (dennis.piontek@dlr.de)

Abstract. Aviation contributes to anthropogenic climate change inter alia through carbon dioxide (CO_2) and nitrogen oxides (NO_x) emissions, as well as contrails. Only a small fraction of flights accounts for a disproportionately large share of the contrail-related CO_2-equivalent (CO_2eq), which might be mitigated through minor, spatially limited flight level adjustments. This study investigates such pre-tactical operational contrail mitigation measures for the full air traffic through Northern Europe for 16 days in 2023, aiming to reduce the sum of CO_2 and non-CO_2 effects. The climate impact assessment follows the European Union's planned monitoring, reporting and verification (MRV) framework for non-CO_2 effects, here employing the 100-year global warming potential (GWP100) as usually applied by the Intergovernmental Panel on Climate Change (IPCC). On average, CO_2 and non-CO_2 effects contribute equally to the total CO_2eq, with contrails and NO_x having similar magnitudes. Weather-related uncertainties from the ECMWF ERA5 reanalysis ensemble are found to be comparably small. Only $6\,\%$ of the flights caused $80\,\%$ of the cumulative contrail-induced CO_2eq. Trajectory adaptations could reduce about $48\,\%$ of the contrail effect in this study, at the cost of a fleet-wide fuel increase of circa 0.4 %. $40\,\%$ of the contrail effect could be avoided when limiting to fuel burn changes per optimized flight to $< 5\,\%$ or meteorological uncertainties $< 20\,\%$. Approximately 28 % of the contrail effect could be mitigated without changes to the fleet-wide fuel burn due to the presence of apparently non-fuel-optimal flight plans in the original air traffic dataset. On specific days, particularly during nighttime, fractions of rerouted flights reached up to 17 %. However, only in the domains of 3 out of 11 air navigation service providers were high total contrail CO_2eq produced simultaneously, showing the spatial limitation of contrail formation areas. While flight altitude changes slightly increase the occurrence of significant air traffic concentrations ($+3\,\%$ for 4-9 aircraft per $2° \times 2° \times 1000\,\mathrm{ft} \times 10\,\mathrm{min}$ grid cell) and of small horizontal separations ($+10\,\%$ for minimal horizontal separations of $5\,\mathrm{NM}$) in this study, the frequencies of these conditions are still comparable to those observed for the original filed flight plans; thus, airspace capacity on average barely limits climate optimization of flights. NO_x-related climate effects were not substantially reduced,

https://doi.org/10.5194/jecats-2026-14
Preprint. Discussion started: 14 August 2026

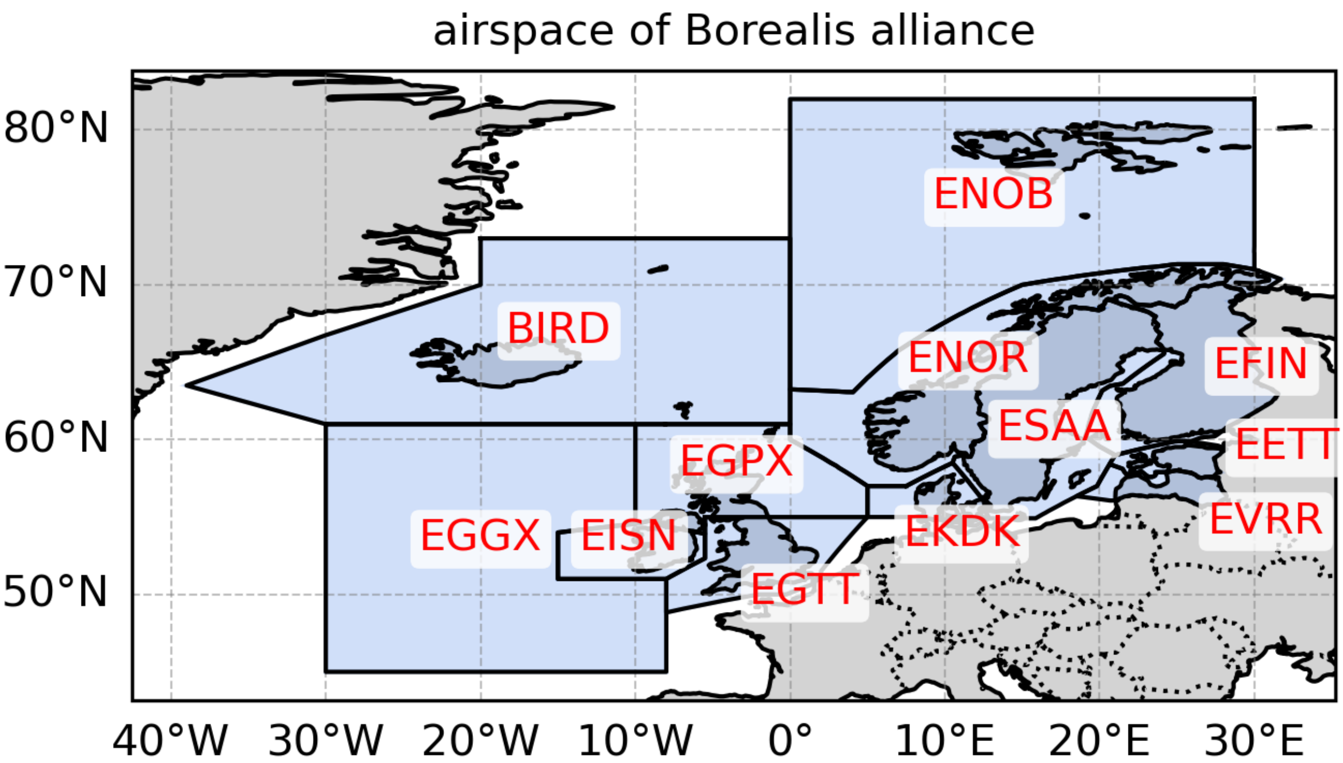

Figure 1. Overview of the airspaces managed by air navigation service providers belonging to the Borealis alliance. Only flights within this combined airspace are optimized in this study.

reflecting their weaker spatial variability. Overall, the results demonstrate the feasibility of pre-tactical air traffic management that avoids airspace regions identified as climate-sensitive by the applied climate assessment framework. While the study is purely model-based and, thus, does not provide an assessment of real-world climate effects, it establishes the concepts and procedures required for the future integration of contrail-avoidance strategies and climate-optimized trajectory planning into operational decision-making and regulatory air traffic management frameworks.

1 Introduction

Aviation contributes to anthropogenic atmospheric warming (Penner et al., 1999), making up about 3.5 % in terms of effective radiative forcing (Lee et al., 2021). This impact is attributed in similar parts to the emission of CO_2, NO_x and contrail cirrus formed from condensation trails, although the strength of the non-CO_2 effects is still relatively uncertain. In particular the need to reduce aviation's non-CO_2 effects—and not only CO_2—has been increasingly recognized in recent years (Arrowsmith et al., 2020), which led to the European Union's establishment of a monitoring, reporting and verification (MRV) system for non-CO_2 effects, potentially leading to legislative measures for their reduction in 2028 (EU Directive 2023/958, 2023).

https://doi.org/10.5194/jecats-2026-14
Preprint. Discussion started: 14 August 2026

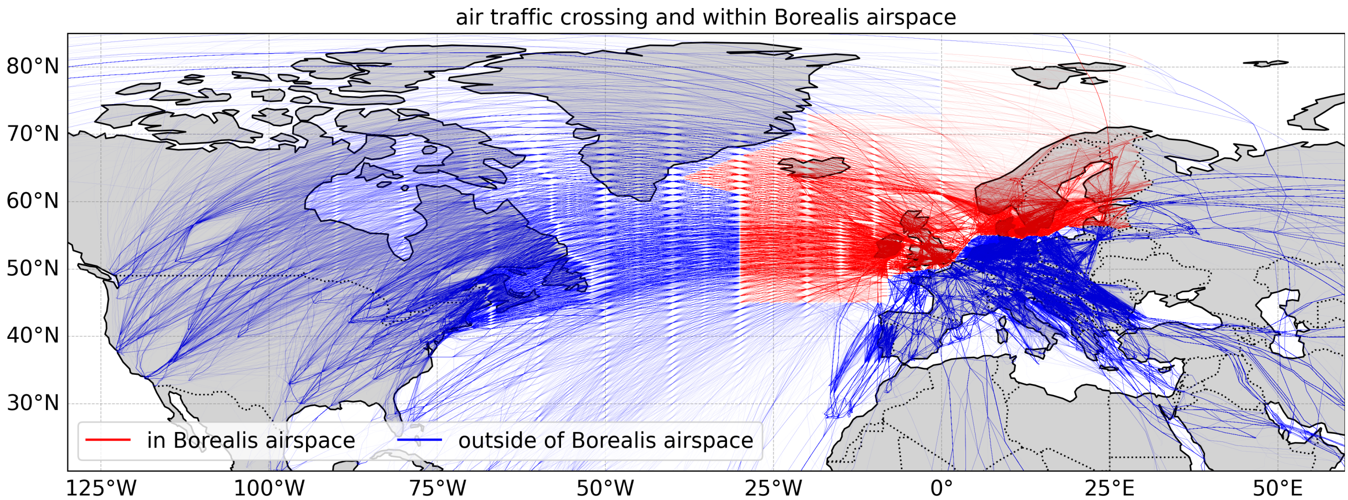

Figure 2. Overview of the air traffic considered in this study, differentiating flight segments within Borealis alliance airspace (red) and external (blue).

Contrails are caused by the emission of water vapor and aerosol particles (e.g., soot) from aircraft engines into sufficiently cold and humid ambient air in order to trigger formation of liquid droplets via condensation and their subsequent freezing to form ice particles (Schumann, 1996; Kärcher, 2018). If the contrail formation takes place in ice-supersaturated regions (ISSRs), the contrail can persist, potentially living more than 10 h (Vázquez-Navarro et al., 2015; Lewellen, 2014) until sedimentation, sublimation, advection and dispersion finally lead to its dissipation (Burkhardt and Kärcher, 2009; Schumann, 2012; Schumann and Heymsfield, 2017). Similar to natural cirrus, contrails reflect incoming shortwave solar light and trap outgoing longwave thermal radiation. The global net radiative effect is positive (Lee et al., 2021), while locally depending on contrail properties, solar insolation, surface properties (e.g. albedo, surface temperature), and particularly the natural ambient cloudiness (Schumann et al., 2012; Wolf et al., 2023). In fact, recent works have indicated that conditions allowing persistent contrail formation exist mainly within subvisible or visible natural cirrus (Petzold et al., 2025), but on average such embedded contrails still have a warming radiative effect (Seelig et al., 2025; Wang and Voigt, 2025).

The aviation-induced climate effect of NO_x emissions is non-linear and therefore highly dependent on the spatio-temporal location and evolution of emission (Dameris et al., 1998). NO_x emissions from aircraft in the upper troposphere and lower stratosphere modify atmospheric ozone (O_3) and methane (CH_4) chemistry through short-term formation of O_3, which has a warming effect, and the depletion of CH_4, which leads to a cooling effect. As a secondary effect, the reduction in ambient CH_4 causes a long-term reduction of O_3, i.e., the primary mode ozone (PMO), and a decrease of stratospheric water vapor, both effects resulting in a long-term cooling. The net NO_x climate effect of these four components is complex, depends on location, season and weather conditions, is subject to strong variability across different models, and is positive on average (Lee et al., 2021; Cohen et al., 2025). Furthermore, there has been a trend of increasing aircraft NO_x emission indices over the last decades

https://doi.org/10.5194/jecats-2026-14
Preprint. Discussion started: 14 August 2026

(Quadros et al., 2022) due to the technology trade-off in gas turbines, where advances have favored higher fuel efficiency at the expense of higher NO_x emissions (Freeman et al., 2018).

There are different options to reduce aviation's climate effect, including improvement of aircraft propulsion system efficiency, development of new engines based on hydrogen combustion or fuel cells, usage of sustainable aviation fuels, or the operational optimization of flight trajectories regarding their climate effect (e.g., Kärcher, 2018; Voigt et al., 2026). Whereas most of these solutions come with long preparation times (e.g., commercial aircraft have life cycles of multiple decades, Penner et al. 1999), operational measures are expected to be feasible within a few years.

The avoidance of contrails is based on the physical properties of ISSRs. Due to their limited horizontal extent (relevant scales of 100 km, Gierens and Spichtinger 2000, see also Vázquez-Navarro et al. 2015; Wolf et al. 2024) and particularly vertical thickness (around 100–1000 m, Spichtinger et al. 2003; Dickson et al. 2009), persistent contrails can be avoided by rerouting aircraft around ISSRs (Mannstein et al., 2005). Depending on the geographical regime, 2–12 % of all flights cause 80 % of the atmospheric contrail impact (Teoh et al., 2020a, 2022a, 2024). A flight altitude change of $\pm$ 2000 ft[1] often already allows significant reductions of the climate effect (Teoh et al., 2020a, b; Matthes et al., 2021; Sausen et al., 2024), with vertical flight adjustments being favored over lateral reroutings (Rosenow et al., 2018; Lührs et al., 2021). As necessary trajectory adaptations to reduce contrail effects can cause increases in flight time and fuel burn, a trade-off (often given as Pareto-fronts) between additional CO_2 emissions and the reduction of contrail-related CO_2eq must be found. The derivation of the latter is sensitive to the choice of the climate metric, e.g., global warming potential (GWP), relative average temperature response (rATR), etc., and the time horizon (Borella et al., 2024), with different choices stressing climate forcers and climate changes slightly differently (Megill et al., 2024; Dahlmann et al., 2025), eventually turning a specific selection into a political decision. However, if strongly warming contrails are formed, their CO_2eq generally overcompensates potential CO_2 costs of flight reroutings independent of the climate metric choice (Kirschler et al., 2026). Consequently, case studies with different modeling setups (including scenarios and climate metrics) find that fleet-wide fuel increases of $< 1\%$ enable reductions of the climate effect by $> 70\%$ for contrails (Teoh et al., 2020b; Martin Frias et al., 2024) or around 50 % for the total climate effect for a day with strong contrail formation (Lührs et al., 2021). In recent years, multiple real world trials have demonstrated the operational feasibility of diverting individual aircraft around airspace marked as contrail-sensitive (Sausen et al., 2024; Sonabend-W et al., 2024; Kirschler et al., 2026; Ehrmanntraut, 2025).

In order to mitigate NO_x climate effects, one can reduce the cruise speed (Simorgh et al., 2022), or fly constantly below the tropopause (Castino et al., 2024). The latter leads to a wider spread of mean flight altitudes and an increase in the lateral flight distance (Castino et al., 2024). However, generally model studies indicate that it is cheaper to reduce the total non-CO_2 climate effect by avoiding warming contrails than by reducing NO_x effects (Castino et al., 2024).

When scaling up operational measures to the full fleet, additional difficulties arise for air traffic management (ATM) in regions with high air traffic density, as avoiding contrail formation lowers the available airspace and, subsequently, increases

[1] Following common standards and practices in the aviation sector, aircraft altitudes and flight levels are given in feet in this work. It holds 1 ft = 0.3048 m (Baucom et al., 2026). A flight level is defined as a surface of constant atmospheric pressure converted to feet assuming standard atmosphere with a surface pressure of 1013.2 hPa and divided by 100 (ICAO, 2024).

https://doi.org/10.5194/jecats-2026-14
Preprint. Discussion started: 14 August 2026

the flight concentrations in neighboring sectors or flight levels, air traffic complexity, and human workload (Andrews et al., 2024). In simulations for the Japanese airspace, slightly less than 14 % of diverted flights experienced a loss of required aircraft separation (Teoh et al., 2020b). The air navigation service provider (ANSP) Maastricht Upper Area Control (MUAC) estimated, in a real-time simulation with human air traffic controllers, a 20 % capacity reduction under normal traffic conditions, and that contrail avoidance might not be feasible in high traffic scenarios (Ehrmanntraut, 2023). In a multi-month tactical real-world trial at MUAC, contrail avoidance through sector clearing was demonstrated to be feasible, although often constrained by ATM capacity limitations (Sausen et al., 2024). Consequently, from an operational perspective, pre-tactical (airline-led) measures might be preferred over tactical ones (Molloy et al., 2022; Ehrmanntraut, 2023), particularly in regions with dense air traffic. However, as contrails interact with each other—directly via radiative transfers (Schumann et al., 2021b; Teoh et al., 2024; Gierens, 2025) or indirectly by competing over available humidity (Burkhardt and Kärcher, 2011; Schumann et al., 2015; Unterstrasser et al., 2017b)—it is currently unclear whether contrails can be treated individually, or whether extended contrail-sensitive airspaces should be cleared; the latter would require a central coordination of flight diversions (Ehrmanntraut, 2025).

Different factors introduce uncertainties in operational measures to avoid contrails. Weather forecasts are imperfect (Wolf et al., 2024, 2025), and in particular (horizontal and vertical) edges of ISSRs are inaccurately predicted (von Bonhorst et al., 2025), although lateral displacements are in the order of one flight-hour (Dean et al., 2025). Usage of generic aircraft/flight settings influences the estimations of potential contrail climate effects used for trajectory optimization (Engberg et al., 2025). Finally, model predictions are uncertain due to their incompleteness regarding physical processes covered and the usage of parameterizations (e.g., Lee et al. (2021) assume an uncertainty of 70 % for contrails). A recently presented risk assessment method by Prather et al. (2025) allows to quantify the chance of mitigation success by taking into account the mitigation potential, its costs, and the before-mentioned model uncertainties; for contrail avoidance, this method indicates a high chance of success (Voigt, 2025). Different future contrail avoidance implementation scenarios were studied by Smith et al. (2026).

This study presents work carried out within the SESAR (Single European Sky ATM Research) project CONCERTO ("Dynamic Collaboration to Generalize Eco-friendly Trajectories"), which aimed at reducing aviation's total climate effect related to non-CO_2 effects by pre-tactical flight plan adaptations at flow level under consideration of meteorological uncertainties and airspace capacity limitations. Focusing on the airspace of the ANSPs organized in the Borealis alliance (see Fig. 1), the full air traffic of 16 representative days in 2023 (see Fig. 2) was climate-optimized. The remainder of this work is structured as follows: Sec. 2 summarizes the assumed concept of operations, datasets and models. Results and their discussion are presented in Sec. 3, including the unoptimized reference situation (i.e., the filed flight plans), the potential of different mitigation strategies and their operational impact. Finally, conclusions are drawn and an outlook is given in Sec. 4.

2 Methods and data

2.1 Concept of operations

Within CONCERTO, a new possible concept of operations was proposed with the goal to reduce the total climate effect (CO_2 and non-CO_2) of the full air traffic in a given airspace. Flight plans would be adapted pre-tactically, i.e., about 3–12 h

https://doi.org/10.5194/jecats-2026-14
Preprint. Discussion started: 14 August 2026

prior to departure and based on initial flight plans of the airspace users (AUs) filed to the network manager (NM, which is EUROCONTROL in the case of Europe). The (automatized) selection of flights to be rerouted would be performed by flow management positions (FMPs) within the individual air navigation service providers (ANSPs), and subsequently the rerouting proposals of affected flights would be communicated to the AUs to update and re-file their flight plans to the NM.

CONCERTO's concept of operations is split in multiple independent tasks. First, so-called "Eco-areas" (i.e., climate-sensitive airspaces) are simulated by climate response models that rely on numerical weather prediction (NWP) data. They are defined as airspaces where the total non-CO_2 effect exceeds a given threshold expressed in global warming potential for a time horizon of 100 years (GWP100), although their occurrence is determined mainly by potential contrail effects (as shown below). Predicting the total non-CO_2 effect for each member of an input data ensemble, an Eco-area certainty is derived as the fraction of simulations exceeding the before-mentioned threshold. Note that our Eco-areas are comparable to the SESAR concept of "environmental hotspots" (which is, however, based on a different contrail model, climate metric and a different, dynamic threshold definition, see ALARM 2022). Second, initial flight plans filed with the NM would be considered and flights that cross an Eco-area are selected. Third, for the selected flights, climate-optimized trajectories are determined. Fourth, savings in the total CO_2eq, i.e., the sum of CO_2 and CO_2eq from non-CO_2 effects, are calculated, considering the weather prediction ensemble to quantify the variability in CO_2eq. Fifth, from the set of identified and rerouted flights, a selection is made by the FMPs, taking capacity consideration and operational constraints into account. This can potentially be automatized based on predefined rules. Sixth, the affected AUs are informed and requested to consider the updated flight plan.

In this study, the following simplifications/specifications of the described concept of operations are made:

– The combined airspace of the ANSPs organized within the Borealis alliance is considered (see Fig. 1). This airspace is suitable as most of them implemented a free route airspace (FRA), many even allowing cross-border FRA operations, allowing more flexible operations as flights are not required to follow a defined route network. Whereas the original motivation for FRA was to increase air space capacity and fuel efficiency (Majka and Pasich, 2022), FRAs are also an important enabler to allow contrail avoidance.

– For the calculation of climate effects, the Contrail Cirrus Prediction Tool (CoCiP, Sec. 2.3.1) is used for contrails and the algorithmic climate change functions (aCCFs, Sec. 2.3.2) for the other gaseous non-CO_2 emissions; this follows the recommended setup for the non-CO_2 MRV (Eichinger et al., 2025). An exception is the sample day selection (Sec. 2.4).

– The calculation of the total non-CO_2 effect and CO_2eq is based on the global warming potential from a pulse emission for a time horizon of 100 years (GWP100, see B), with the non-CO_2 GWP100-threshold for Eco-areas defined as $T_{\mathrm{GWP100}} = 0.995$ (see Sec. 2.4 and compare the approach of Widmaier et al. 2026). Note that also the flight trajectory optimization is influenced by the choice of the climate metric.

– Two different input data ensembles are used: For the Eco-area determination, a 10-member meteorology ensemble (see Sec. 2.2.1), two typical aircraft (A321 with engine 04P10IA027 as a light and B77W with engine 01P21GE217 as a heavy aircraft, see Widmaier et al. 2026) and two headings (northward and eastward) are considered (effectively leading to 40

https://doi.org/10.5194/jecats-2026-14
Preprint. Discussion started: 14 August 2026

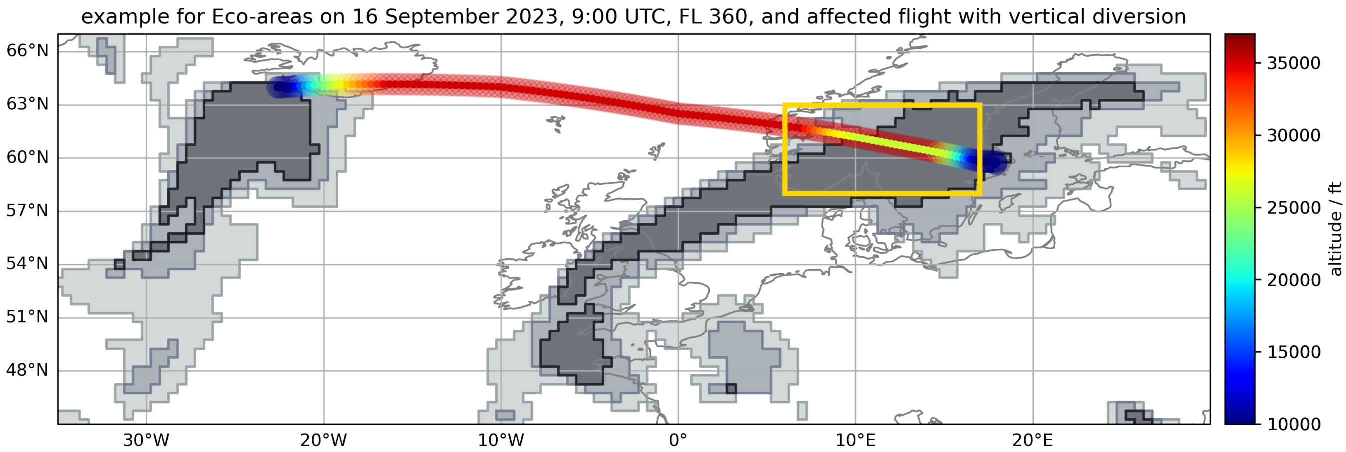

Figure 3. Example showing Eco-areas for 16 September 2023, 9 UTC, at flight level 360 as shaded areas for agreements of 10 % (light grey), 50 % (grey) and 90 % (dark grey) in the 40-member ensemble. The original (bold) and optimized (thin) trajectory for a selected flight from Keflavik (Iceland) to Stockholm (Sweden) is shown, with the altitude indicated by the color. Due to an extended Eco-area covering large parts of Southern Sweden, Norway and extending all the way across the United Kingdom, the flight performs an early descend to dive under the Eco-area in the area indicated by the rectangle.

members), comparable to the approach by Engberg et al. (2025). For the flight-specific evaluation, only the 10-member meteorology ensemble is considered (aircraft type and heading are well-defined in this case).

- Following a conservative approach to keep the amount of missed mitigation opportunities minimal, flights are selected based on Eco-areas with 10 % certainty, i.e., at least 4 out of 40 ensemble members must predict an Eco-area at a given point.
- No operational or capacity constraints from FMPs are considered during the selection of flights for optimization.

An example for different Eco-areas and a flight that experiences a rerouting is shown in Fig. 3.

2.2 Data

2.2.1 Meteorology

Climate effects are simulated by response models based on the ECMWF (European Centre for Medium-Range Weather Forecasts) ERA5 10-member reanalysis ensemble (Hersbach et al., 2020). It has a horizontal resolution of 0.5° × 0.5°, consists of 37 pressure levels, and is available every 3 hours; thus, it is lower resolved than the single ERA5 hourly, high resolution realization. As NWP models still have problems in accurately and consistently representing ice supersaturated regions (e.g., Gierens et al., 2020; Wolf et al., 2025; Dischl et al., 2022; Wang et al., 2025), a correction of the relative humidity is needed. Here, the humidity scaling of Teoh et al. (2022a) based on a comparison with in-situ measurements from IAGOS (In-service Aircraft for a Global Observing System) is applied (with $a = 0.9779$, $b = 1.635$ and an upper clipping of 1.65, see their Eq. 1).

https://doi.org/10.5194/jecats-2026-14
Preprint. Discussion started: 14 August 2026

2.2.2 Air traffic

Actual flight plans filed to EUROCONTROL were collected. They were converted to flight trajectories using aircraft performance calculations based on EUROCONTROL's base of aircraft data (BADA3) with standard mass assumptions (EUROCONTROL, 2022). Only flights which at least partially traverse the Borealis alliance airspace at the study dates ± 24 h were selected. Given typical ISSR and contrail sizes and aircraft cruise speeds, the flight trajectories are upsampled to a temporal resolution of 60 s to resolve contrail formation along the flight path (Schumann et al., 2021b; Teoh et al., 2022a). Based on trajectory start and end points, callsigns and aircraft types, multiple filters were applied to remove potentially duplicated flight plans (A).

Note that this air traffic data—in contrast to, for example, ADS-B (automatic dependent surveillance – broadcast) data—does not represent actually flown trajectories and, thus, does not include trajectory alterations due to operational impacts (e.g., delayed aircraft takeoffs, directs offered tactically to the pilots by air traffic controllers, flight reroutings due to unpredicted severe weather events). Thus, our air traffic data differs from actual historical flight data as often used in other studies (Schumann et al., 2021a, b; Teoh et al., 2022a, 2024; Borella et al., 2024).

2.3 Models

2.3.1 Contrail Cirrus Prediction Tool (CoCiP)

The Contrail Cirrus Prediction Tool (CoCiP) is a Lagrangian contrail plume model including various physical processes in parametrized form, and based upon meteorological data, flight trajectories and settings including aircraft, engine and fuel type (Schumann, 2012). First, the aircraft performance (including fuel burn and engine efficiency) along the flight trajectory is simulated using the base of aircraft data (BADA3) performance tables (EUROCONTROL, 2022). Second, emissions of non-volatile particle matter (nvPM) are calculated from the fuel burn and the ICAO aircraft engine emission databank (EDB) when covered, alternatively using approximations based on the gaseous emissions covered by the ICAO EDB or constants (Teoh et al., 2022b, a; Stettler et al., 2013; Abrahamson et al., 2016). Here, Jet A1 fuel is assumed for all flights. Third, for each flight segment a contrail is formed if the Schmidt-Appleman criterion (SAC) is fulfilled (Schumann, 1996). Fourth, the wake vortex downward motion is considered with a parameterization of the probabilistic two-phase vortex decay and transport model of Holzäpfel (2003) and spatial displacements due to wind shear. A Gaussian concentration profile is assumed, whose position, size and shape can change over the contrail's lifetime. Fifth, the initial ice water content and the ice particle number are estimated, taking adiabative heating, particle loss processes and limited ice activations in parameterized form into account (Schumann, 2012; Bräuer et al., 2021). Sixth, the further development of the contrail's micro- and macrophysical properties takes place iteratively (here with a timestep of 30 min) by advection and wind shear within the 4D meteorological fields and using parameterizations of particle sedimentation, aggregation and sublimation (Schumann, 2012). The contrail reaches its end of life when it reaches a predefined age (here set to 12 hours), or if one of its microphysical, macrophysical or radiative properties lies outside predefined, physical ranges. Finally, the atmospheric impact is evaluated by calculating the contrail-related net local radiative effect, i.e., the instantaneous change in the local radiative energy balance, using a parameterization

https://doi.org/10.5194/jecats-2026-14
Preprint. Discussion started: 14 August 2026

(Schumann et al., 2012) of the radiative transfer model libRadtran (Mayer and Kylling, 2005). The time integral of the product of local radiative forcing (RF) and contrail size is called energy forcing (EF) and attributed to the producing flight segment.

Instead of this trajectory-based application, the CoCiP model can also be applied to small, generic flight segments at each point of a 4D grid, effectively producing a scalar field of potential contrail impacts (Engberg et al., 2025) that can be used to identify climate-sensitive airspaces (here Eco-areas) or to optimize flight trajectories.

Notable limitations of CoCiP include neglected radiative interactions between contrails in the grid mode (Schumann et al., 2021b; Teoh et al., 2024; Gierens, 2025), missing humidity feedbacks affecting both the interaction between contrails (Schumann et al., 2015) and between contrails and natural cirrus (Burkhardt and Kärcher, 2011; Unterstrasser et al., 2017b). The high degree of parametrization of physical processes in CoCiP–compared to, for instance, large eddy simulations (Lewellen et al., 2014; Lewellen, 2014; Unterstrasser et al., 2017a, b)–might cause non-negligible inaccuracies. When comparing CoCiP against the higher-fidelity Aircraft Plume Chemistry, Emissions, and Microphysics Model (APCEMM), Akhtar Martínez et al. (2025) found 3.8 times larger time-integrated total extinctions for APCEMM, and opposite sensitivities with respect to the relative humdity. Despite that, CoCiP has been thoroughly compared with ground cameras (Schumann et al., 2013), satellite observations (Schumann and Graf, 2013; Schumann et al., 2017, 2021a, b; Schumann and Heymsfield, 2017; Teoh et al., 2024; Wang et al., 2025), and in-situ measurements (Voigt et al., 2010, 2022; Harlass et al., 2024; Dischl et al., 2024; Märkl et al., 2024).

Here, CoCiP is used as implemented in the Python package pycontrails version 0.50.2 (Shapiro et al., 2023) together with the BADA-wrapper pycontrails-bada version 0.5.3.

2.3.2 Algorithmic climate change function (aCCF)

Algorithmic climate change functions (aCCFs) are weather-dependent response functions that approximate the spatially and temporally resolved climate effect of aviation emissions over the North Atlantic flight corridor (NAFC) at cruise altitudes (van Manen and Grewe, 2019; Yin et al., 2023; Dietmüller et al., 2023). They were derived by statistical fits to climate change functions (CCFs) that were calculated by computationally demanding climate–chemistry simulations using Lagrangian methods (Grewe et al., 2014; Frömming et al., 2021). The currently available prototype aCCFs are computationally light and available for relevant non-CO_2 emissions, i.e., NO_x-induced O_3 and CH_4, H_2O, and contrails. The current aCCF formulation is based on five typical winter and three summer weather patterns within the NAFC for pressure levels between 200-400 hPa (Frömming et al., 2021; Yin et al., 2023); the usage of the aCCFs elsewhere and for other seasons is an off-design application, potentially limiting their accuracy. Here, we limited our investigation to the vertical extent of 150-400 hPa. The climate response of gaseous non-CO_2 emissions was assumed to be zero at pressures $>$400 hPa and $<$150 hPa; the same limitation was applied to CoCiP results to enable a fair comparison of contrails and other non-CO_2 effects. Following the current recommendations for the non-CO_2 MRV (Eichinger et al., 2025), the aCCFs for NO_x and H_2O are used in version 1.0A which includes factors to align original aCCF results to the considerably lower values of the climate response model AirClim (Simorgh et al., 2024), whereas for contrail effects the original CoCiP version (without alignment to a climate model) is applied. We use the open-

https://doi.org/10.5194/jecats-2026-14
Preprint. Discussion started: 14 August 2026

source Python library CLIMaCCF (Dietmüller et al., 2023), which provides an implementation of the aCCFs, using its version dated 6 September 2024 (GitHub commit 6d5696a).

2.3.3 Flight trajectory optimizer

Generally, two different approaches for a trajectory optimization are possible: minimization of a cost function including CO_2 and non-CO_2 effects, or defining airspaces which should be completely avoided (Niklaß et al., 2019; Engberg et al., 2025). Here, we follow an intermediate approach using a very simple experimental trajectory optimizer. For a flight crossing an Eco-area, its corresponding entry and exit points along the trajectory are determined. Up to 100 alternative trajectories are created with local vertical deviations to lower flight altitudes, varying a) the start and end points of the rerouting, and b) the altitude to which the flight is lowered. For each alternative trajectory, the cost function c is evaluated between the entry and exit point,

$$c = d_{\text{Eco-area}} - k \cdot h_{\text{mean}} \cdot d_{\text{total}}, \tag{1}$$

with the mean flight altitude h_{mean}, the total distance of the flight trajectory d_{total}, and the flight distance crossing the Eco-area $d_{\text{Eco-area}}$. The factor $k = 1.6 \times 10^{-4}\,\text{m}^{-1}$ was selected by manual fine tuning to achieve a trade-off between the avoidance of the Eco-area and flying at higher, more fuel-efficient flight altitudes. The trajectory with the lowest cost c is accepted if the fuel burn increase stays below 2 %, otherwise no trajectory optimization is conducted.

2.4 Sample selection

We identified a set of 16 sample days in the form of 8 consecutive two-day blocks distributed throughout the year 2023 (see Table 1). Blocks of 48 h were chosen to include full flights during day and night, such as overnight trans-Atlantic flights. The selection considers different seasonality (summer months including May to September, and winter months including November to March), type of day (weekday, weekend), and daily climate effect scenarios ("normal", "large"; see definition below). In order to select these days, we analyzed 4 full months (March, June, September, December) of Borealis air traffic in 2023. Flight numbers in the Borealis area show seasonal variability: In summer (June, September), daily flights averaged to 11151 and 9621, respectively, while in winter (March, December) they averaged to 8085 and 8184. Weekdays experienced higher air traffic than weekends for three months (June, September, December), with significant differences in June. During March, weekends were slightly busier than weekdays. The two climate effect scenarios refer to days in which the total length of all simulated flight segments exceeding a non-CO_2 GWP100 of $T_{\text{GWP100}} = 0.995$ is close to the monthly mean ("normal") or exceeds it significantly ("large"). For a robust selection, we chose sample days for normal and large climate effects based on the qualitative agreement of two different modeling approaches for the climate effect: Approach (1) uses CoCiP for contrails and additionally the NO_x and H_2O aCCFs for gaseous non-CO_2 emissions, the BADA3 aircraft performance model (EUROCONTROL, 2022), and the climate metric GWP100 for pulse emissions. Approach (2) uses the aCCFs for both contrails and NO_x, the Poll-Schumann aircraft performance model (Poll and Schumann, 2021), and the climate metric rATR20 for pulse emissions. Both approaches use deterministic ECMWF ERA5 reanalysis data (in contrast to the meteorology ensemble data used otherwise in

https://doi.org/10.5194/jecats-2026-14
Preprint. Discussion started: 14 August 2026

this work, see 2.2.1) and air traffic data within a rectangular boundary box covering Borealis alliance airspace, resampled to one minute resolution (see 2.2.2).

Approach (1) also allowed to derive the non-CO_2 GWP100 threshold T_{GWP100} as the 20 % percentile (an ad hoc decision based on reports of similar quantiles in Teoh et al. 2020a, 2022a, 2024) of the cumulative non-CO_2 GWP100 (including positive and negative effects) of all simulated flight segments of the full 4 months for the complete Borealis domain. Using the same simulations, weights were determined to approximate weighted averages for the full year (see Table 1). Each weight denotes the fraction of days within the considered 4 months that are represented by a sample day based on the similarity of the corresponding flown distances above T_{GWP100}. Note that this weighted average might slightly overestimate annual results as days with particularly small climate effects are not considered specifically.

#	Season	Day	Climate effect	Selected days	Weight
1	Summer	Weekday	Normal	June 7	0.197
				June 8	0.082
2	Summer	Weekday	Large	June 13	0.016
				June 14	0.09
3	Summer	Weekend	Normal	Sep 2	0.041
				Sep 3	0.016
4	Summer	Weekend	Large	Sep 16	0.025
				Sep 17	0.025
5	Winter	Weekday	Normal	Dec 27	0.041
				Dec 28	0.098
6	Winter	Weekday	Large	Dec 21	0.041
				Dec 22	0.008
7	Winter	Weekend	Normal	Mar 18	0.213
				Mar 19	0.074
8	Winter	Weekend	Large	Dec 16	0.016
				Dec 17	0.016

Table 1. Selected sample days varying in seasonality ("summer" covers May to September and "winter" the months November to March), type of day (weekday or weekend, with weekdays tending to have increased air traffic volume), and climate effect ("normal" denotes days with typical climate effect, "large" indicates unusually high climate effect, see text). Two consecutive days (48h) in 2023 were selected per case. For each day, a weight is provided to determine a weighted mean as an estimate for the annual average.

https://doi.org/10.5194/jecats-2026-14
Preprint. Discussion started: 14 August 2026

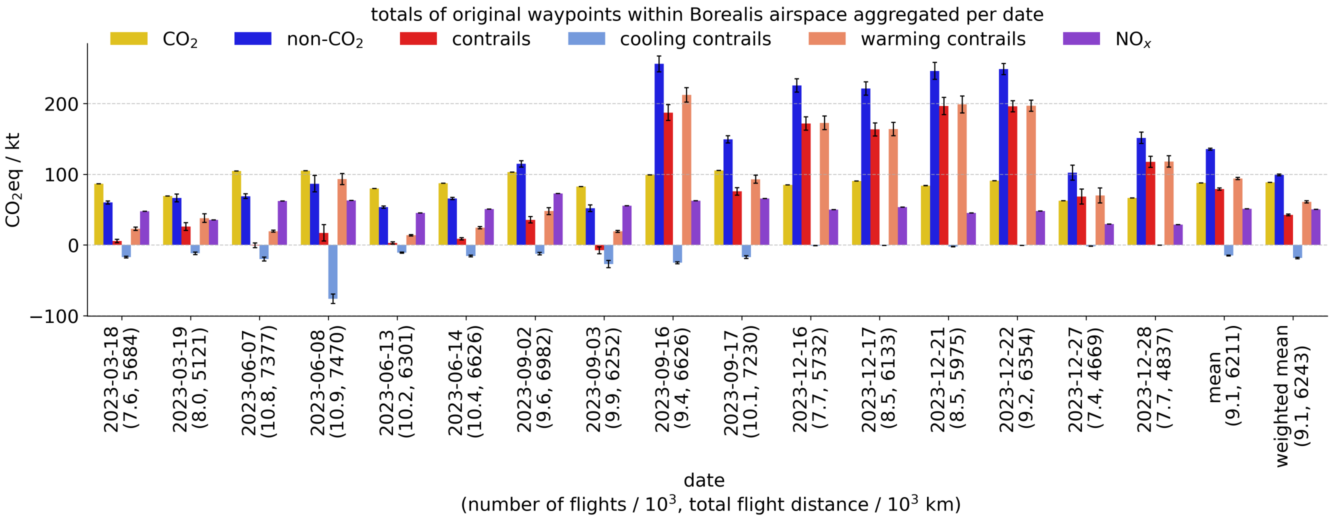

Figure 4. 10-member ensemble mean CO_2 and CO_2eq emissions per date from all waypoints within the Borealis alliance airspace for the original air traffic. The contrails bars represent the sum of warming and cooling contrails, and the non-CO_2 bar shows the sum of contrails, NO_x and H_2O. The uncertainty range indicates the 95 % confidence interval of the mean for the 10-member meteorology ensemble.

3 Results and discussion

3.1 Reference situation

In total, the comprehensive set of 145092 flights with at least one trajectory waypoint within Borealis alliance airspace at the study dates are considered as a reference. Of those flights, 19.4 % completely stay within the Borealis alliance airspace, whereas 80.6 % enter and/or leave it. Consequently, 29.1 % of all waypoints are located inside and 70.9 % outside of Borealis alliance airspace (compare Fig. 2). Therefore, we differentiate in the evaluation between an ANSP perspective (considering only waypoints within Borealis alliance airspace at the study dates, taking incomplete flight trajectories into account) and an AU perspective (considering all waypoints of flights with at least one waypoint inside the Borealis alliance airspace at the study dates); thus, in the AU perspective also waypoints outside the Borealis alliance airspace or at days before or after the selected study days might be included.

3.1.1 ANSP-perspective

The CO_2eq emissions per date and per species are shown in Fig. 4. The forcers show different temporal variability and effect: The effects from CO_2 and NO_x vary only slightly as they depend mainly on the number of flights/the total flight distance; additionally, the effectiveness of the NO_x climate effect has a weak seasonal dependence (Castino et al., 2021), see also D. Contrails vary strongly between around 0 kt and 200 kt, indicating that contrails are also the main factor in the definition

https://doi.org/10.5194/jecats-2026-14
Preprint. Discussion started: 14 August 2026

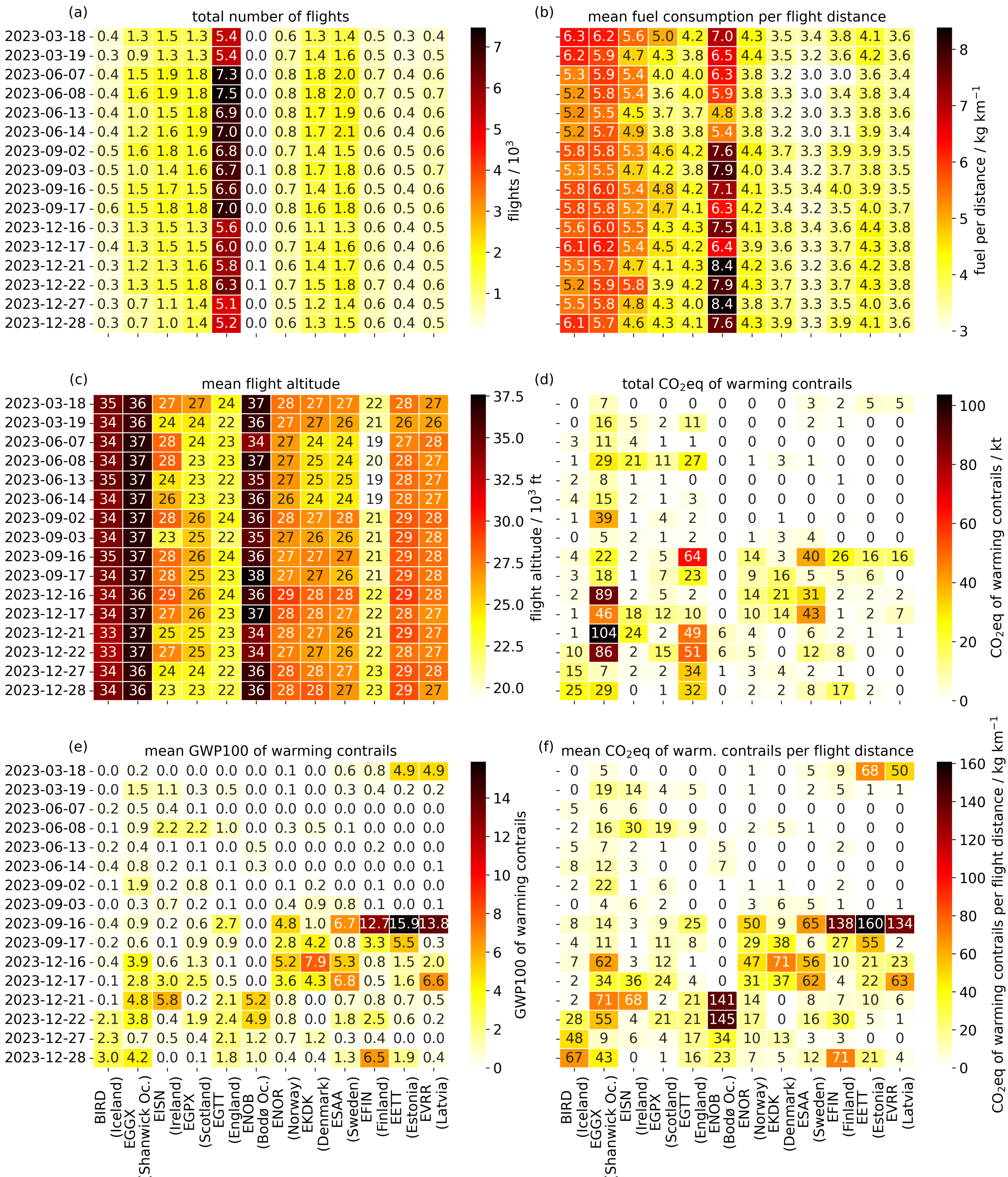

Figure 5. Heatmaps based on all waypoints in the original air traffic within Borealis alliance airspace at the study days, showing a) the total number of flights, b) the mean fuel consumption per flight distance, c) the mean flight altitude, d) the total CO_2eq from warming contrails, e) the mean GWP100 of warming contrails, and f) the mean CO_2eq of warming contrails per flight distance.

https://doi.org/10.5194/jecats-2026-14
Preprint. Discussion started: 14 August 2026

of the Eco-areas. The weighted annual means are $(88.6202 \pm 0.0006)\,\mathrm{kt\,d^{-1}}$ for CO_2, $(42.5 \pm 0.5)\,\mathrm{kt\,d^{-1}}$ for contrails, and $(50.508 \pm 0.002)\,\mathrm{kt\,d^{-1}}$ for NO_x, showing that the combined non-CO_2 effect has about the same size as the CO_2.

The study days 16–17 September, 16–17 December, 21–22 December show significantly larger contrail effects than the rest of the study periods which agrees with their initial classification, see Table 1. The fourth period initially predicted to have a large climate effect (13–14 June) actually has a contrail effect close to zero (Fig. 4). This might be explained by the fact that the initial classification in the sample selection was based on deviations from monthly averages, with summer season being overall less favorable for persistent, strongly warming contrails (Teoh et al., 2022a, 2024; Dischl et al., 2022; Kaufmann et al., 2024). During the days in spring, summer and fall both warming and cooling contrails are produced, whereas nearly no cooling contrails are produced at the days in December. For the 3 September, the net contrail effect is cooling for the complete confidence interval, whereas the confidence interval includes positive and negative values for 7 June. Generally, the confidence interval of the contrail mean impact is notably larger than for CO_2 and NO_x but still remains small relative to the contrail mean impact for the study periods in late-September and December (around 10 %).

As the contrail climate effect has the largest variability, the temporal and spatial distribution of the effect of warming contrails in the ANSP sectors is shown in Fig. 5. During the days with large climate effect in late-September and December, the largest contributions in terms of total CO_2eq from warming contrails come from only few airspaces (Shanwick Oceanic, EGGX; England, EGTT; Sweden, ESAA). Other airspaces are hardly affected during this time, e.g., Bodø Oceanic (ENOB), whereas Estonia (EETT) and Latvia (EVRR) have significant contributions only on 16 September. Whereas the high impact for England coincides with the fact that this airspace experiences the most flights (see Fig. 5a), this argument does not hold for Shanwick Oceanic. Instead, the combination of the localized presence of conditions favoring persistent and strongly warming contrails and the typical high flight altitudes for a large fraction of the cross-Atlantic air traffic (see Fig. 5c) most likely explains the strong impact over the Atlantic airspace. For example, Teoh et al. (2024) modeled that globally the North Atlantic flight corridor has the highest ratio of energy forcing to total flight distance. If the CO_2eq from warming contrails is normalized with the flight distance (see Fig. 5f), other sectors stand out, including Finland (EFIN), Estonia (EETT) and Latvia (EVRR) on 16 September and Bodø Oceanic (ENOB) on 21-22 December, indicating that the few flights in those domains produce very high contrail climate effects. When normalizing the CO_2eq from warming contrails with the CO_2 emission (corresponds to GWP100, see Fig. 5e), the situation is similar, although Bodø Oceanic (ENOB) has only an average value in this metric due to the extraordinary high mean fuel consumption per flight distance (see Fig. 5b). Although it cannot be concluded that certain Borealis alliance airspaces are more susceptible for strongly warming contrails from this study, Fig. 5d demonstrates that typically only a fraction of its airspace is affected at the same time.

3.1.2 AU-perspective

Fig. 6 shows the normalized cumulative distributions of CO_2eq against the fraction of all flights, and against the fraction of the total flight distance. The main contribution from CO_2, NO_x and contrails are caused only by a fraction of the flights. However, those are not necessarily the same flights (distributions are sorted separately in Fig. 6). Considering the CO_2eq relative to the flight distance, the contributions from CO_2 and NO_x are much more homogeneously distributed over all flight distance. Thus,

https://doi.org/10.5194/jecats-2026-14
Preprint. Discussion started: 14 August 2026

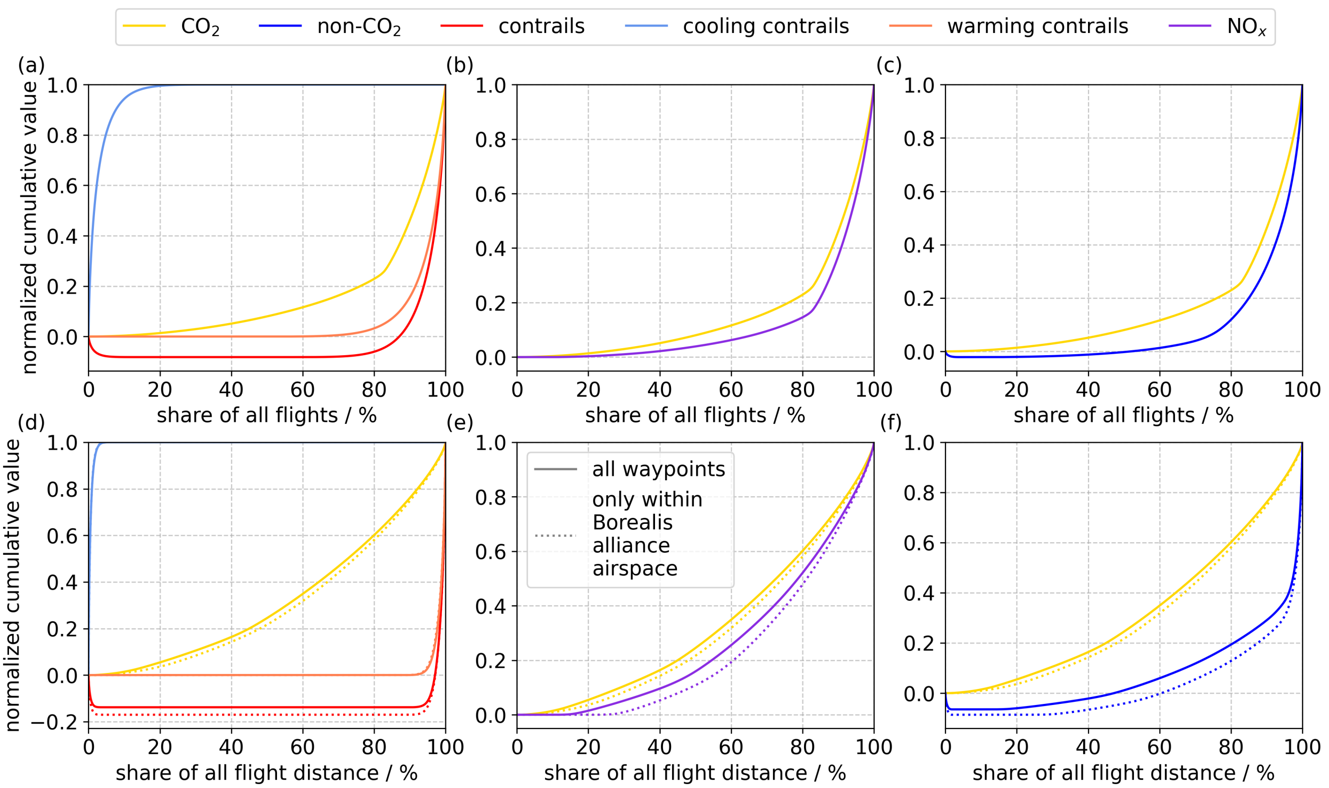

Figure 6. Normalized cumulative values for CO_2eq per fraction of all flights with at least one waypoint within the Borealis alliance during the study periods for the original air traffic (upper row) and per fraction of total flight distance for the same set of flights (lower row). Each species is sorted individually (i.e., the flight with the highest contrail climate effect not necessarily has also the highest NO_x climate effect). The graph for cooling contrails is positive due to its normalization.

the fact that 80 % of the CO_2 and NO_x emissions are caused by 24 % and 16 % of all flights, respectively, is explained mainly by the fact that these are long-haul flights, burning large amounts of fuel and, thus, producing large amounts of CO_2 and NO_x. This cannot easily be mitigated. It also shows that aviation climate effects should always be evaluated relative to the flight distance (or fuel burned) when comparing the different non-CO_2 effects.

For contrails, the situation is different: Around 20 % of the flights produce significantly cooling and 30 % produce warming contrail segments. 80 % of the total contrail CO_2eq is caused by only 6 % of the flights. This agrees quantitatively with similar attributions of 12 % of all flights when considering the North Atlantic (Teoh et al., 2022a) and 2 % globally (Teoh et al., 2024) when considering cumulative energy forcing (which is proportional to our CO_2eq definition, see B). With respect to the overall flight distance, < 2 % cause 80 % of the total contrail CO_2eq. The attribution of the contrail climate effect to only few flights/flight segments also allows an effective contrail avoidance with only limited operational costs.

https://doi.org/10.5194/jecats-2026-14
Preprint. Discussion started: 14 August 2026

Flight type	Climate effect	Flight distance / km	Share of flights / %	CO_2eq / t	GWP100	CO_2eq/dist. / kg km^{-1}
			CO_2			
long-haul	/	7659	19.4	158.4	1	20.1
medium-haul	/	2288	30.9	20.5	1	8.9
short-haul	/	798	49.7	6.8	1	8.3
			Contrails			
long-haul	large	7203	2.3	623 ± 13	5.6 ± 0.1	86 ± 2
long-haul	medium	7690	13.8	53 ± 1	0.30 ± 0.01	6.6 ± 0.1
long-haul	small	7847	3.3	-47 ± 2	-0.31 ± 0.01	-6.1 ± 0.3
medium-haul	large	2355	5.3	222 ± 8	10.8 ± 0.4	98 ± 4
medium-haul	medium	2274	20.2	4 ± 0.2	0.18 ± 0.01	1.62 ± 0.09
medium-haul	small	2272	5.4	-19 ± 1	-0.99 ± 0.05	-8.9 ± 0.4
short-haul	large	1002	4.9	104 ± 6	11.1 ± 0.6	99 ± 5
short-haul	medium	749	41.0	0.8 ± 0.04	0.086 ± 0.004	0.79 ± 0.04
short-haul	small	1065	3.8	-11 ± 0.8	-1.12 ± 0.09	-9.6 ± 0.7
			NO_x			
long-haul	large	8108	10.3	157	0.8	19
long-haul	medium	7153	9.0	78	0.6	10
long-haul	small	6172	0.1	3	0.1	0.4
medium-haul	large	2590	1.8	20	0.8	7
medium-haul	medium	2270	28.9	10	0.5	4
medium-haul	small	2112	0.2	0.4	0.1	0.2
short-haul	large	1209	0.4	5	0.7	4
short-haul	medium	930	37.1	3	0.4	3
short-haul	small	388	12.3	0.1	0.02	0.2

Table 2. 10-member ensemble mean per flight for the CO_2eq, the CO_2eq per CO_2 emission (equals GWP100), and the CO_2eq per flight distance. Considered are all waypoints of flights with at least one waypoint inside the Borealis alliance airspace at the study days for the original air traffic. The uncertainty range indicating the 95 % confidence interval of the mean for the 10-member meteorology ensemble is given for contrails only as weather-related uncertainties are 2 or more orders of magnitude smaller than the means for CO_2 and NO_x. Flights are grouped per type according to their flight distance following EUROCONTROL (2011) ("long-haul": $> 4000\,\mathrm{km}$, "medium-haul": 1500–4000 km, "short-haul": $< 1500\,\mathrm{km}$), and their GWP100 ("large": $> 87.5\,\%$ percentile, "medium": between 12.5 % and 87.5 % percentile, "small": $< 12.5\,\%$ percentile; percentiles determined species-specific). The share of flights and a mean flight distance are given per category.

https://doi.org/10.5194/jecats-2026-14
Preprint. Discussion started: 14 August 2026

Table 2 shows mean values for the per flight CO_2eq as well as CO_2eq per fuel burned and per flight distance. Flights are grouped based on their flight distance (short-, medium- or long-haul) and their GWP100 (small, medium or large climate effect); see caption of Table 2 for definitions. The CO_2 emission per flight distance agree well with literature values, e.g., a long-haul A350-900 flight has a fuel burn of approximately $6.5\,\mathrm{kg(fuel)\,km^{-1}}$ (Aircraft Commerce (2018); corresponds to $20.5\,\mathrm{kg(CO_2)\,km^{-1}}$; here $20.1\,\mathrm{kg(CO_2)\,km^{-1}}$) and a short-haul A319 burns $2.9\,\mathrm{kg(fuel)\,km^{-1}}$ (Aircraft Commerce (2005); equals $9.2\,\mathrm{kg(CO_2)\,km^{-1}}$; here $8.3\,\mathrm{kg(CO_2)\,km^{-1}}$). Regarding NO_x, Table 2 shows again a strong dependence on the flight distance: most flights with large climate effect are long-haul flights, whereas most flights with small climate effect are short-haul flights. Also the NO_x-related CO_2eq per flight distance increases from short- to long-haul flights, caused by differences in typical flight altitudes and aircraft types. However, for contrails we find that small and large climate effects are relatively equally distributed between short- to long-haul flights. Also, the contrail-related CO_2eq per flight distance remains relatively constant (same order of magnitude) for flights with large/small climate effect but different flight lengths; amplitudes for CO_2eq per flight distance are largest for short-haul flights. Cooling contrails occur with similar frequency for all flight lengths. Overall, Table 2 shows that for contrails the absolute effects increase in amplitude with flight length (i.e., longer flights produce more contrail-related CO_2eq), whereas the normalized effects decrease (i.e., shorter flights are more efficient in producing contrail-related CO_2eq emission).

3.2 Mitigation strategies

In the following, the consequences of an optimization of the full air traffic are discussed, focusing on reductions in the climate effect and on operational impacts (including amount of flight plan modifications, airspace congestion, and aircraft separations).

3.2.1 Climate effect

Based on the Eco-areas, about 12.8 % of all flights were selected and a climate-optimized trajectory was derived by avoiding these Eco-areas. Reevaluating these trajectories with flight-specific model calculations showed that the total CO_2eq was reduced for all members of the 10-member meteorology ensemble for 46 % of the optimized flights, and reduced in some of the ensemble members in additional 39 % of the cases. This demonstrates the robustness of the investigated mitigation approach despite the simplicity of the concept of operations and the trajectory optimization, as well as the limitations of the applied climate response models.

The CO_2eq was reduced in none of the ensemble members only for 15 % of the optimized flights. This can be explained by the usage of generic climate effect field calculations instead of flight-specific properties such as the aircraft type (in particular due to the conservative approach pursued here by considering Eco-areas with 10 % certainty, see Sec. 2.1) or the fuel burn. Additionally, the selection of flights and their trajectory optimization was performed based on the Eco-areas, which were derived with a temporal resolution of 3 hours (i.e., the temporal resolution of the meteorological data) and kept spatially fixed in the meantime. In contrast, the flight-specific simulation of non-CO_2 effects was based on the same meteorological data which, however, was linearly interpolated both spatially and temporally to the flight waypoints. This difference can lead to cases in which a flight is assumed to cause a significant non-CO_2 effect (i.e., it crosses an Eco-area) but the more accurate

https://doi.org/10.5194/jecats-2026-14
Preprint. Discussion started: 14 August 2026

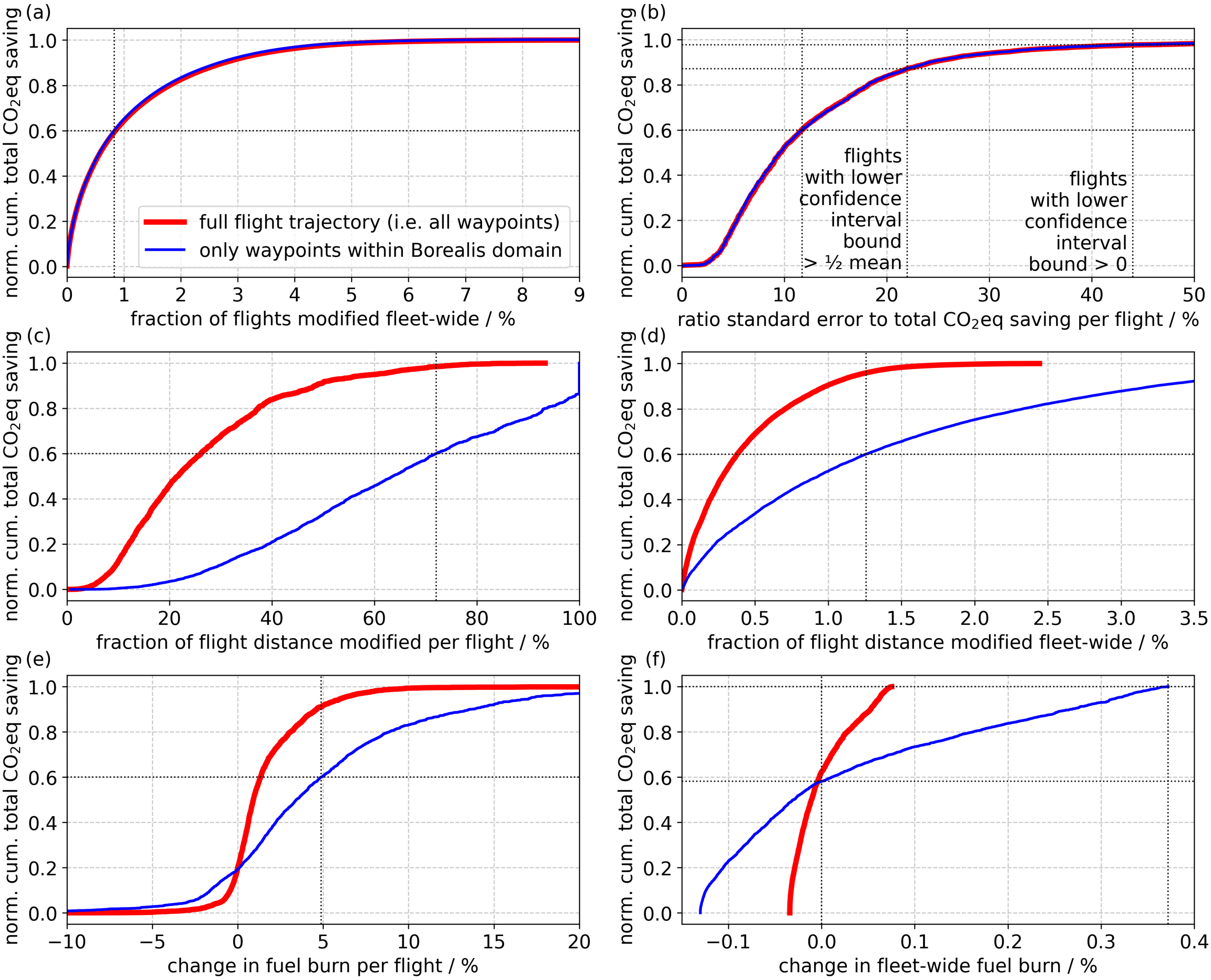

Figure 7. Normalized cumulative total CO_2eq saving using the full optimization with respect to a) the fraction of optimized flights, b) the standard error divided by the mean of the total CO_2eq saving per optimized flight, c) the fraction of flight distance modified per optimized flight, d) the fraction flight distance modified relative to the flown flight distance of all flights, e) the mean in the relative change in fuel burn per optimized flight, f) the relative change in fleet-wide fuel burn. Distributions are shown for the full flight trajectories including waypoints outside Borealis alliance airspace (red) and for the subset of waypoints inside Borealis alliance airspace (blue). Black dotted lines indicate specific points mentioned in the text. Curves shown for fleet-wide estimates (a, d, f) depend on the ordering of the individual elements in the fleet before calculating cumulative values; they are ordered starting with the highest mitigation potential (a, d) or the lowest fuel burn increase (f).

https://doi.org/10.5194/jecats-2026-14
Preprint. Discussion started: 14 August 2026

flight-specific simulation of its non-CO_2 effect does not confirm this. A more effective selection of flights for optimization as well as trajectory optimization might affect the numbers above and the mitigation potentials presented in the following.

In the remainder, we consider only trajectory optimizations that reduce the mean total CO_2eq across the 10-member meteorology ensemble (9 % of all flights, called "full optimization" in the following). Fig. 7 shows the achievable mitigation potential depending on different quantities; we focus only on waypoints within the Borealis domain in the following. Even within the 9 % of flights optimized, only a subset produces the major share of CO_2eq: Optimizing just 1 % of all flights already allows to achieve $> 60\,\%$ of the mitigation potential (Fig. 7a). The fraction of flight distance that needs to be modified per optimized flight is not limited, but at least circa 10 % of the flight distance needs to be modified to realize a notable mitigation (Fig. 7c). Relative to the whole fleet (i.e., including all optimized and unoptimized flights), about 1.25 % of the overall flight distance needs to be optimized to achieve 60 % of the mitigation potential (Fig. 7d). Limiting fuel burn changes to $\leq 4.9\,\%$ per optimized flight also allows to achieve 60 % mitigation potential (Fig. 7e), consistent with reported per-flight fuel penalties of 2–5 % in comparable contrail mitigation studies (Engberg et al., 2025; Kirschler et al., 2026). Notably, some flights exhibit negative fuel burn changes (i.e., fuel savings due to rerouting), likely reflecting non-fuel-optimal original trajectories caused by operational constraints. Consequently, presented results might overestimate the mitigation potential as fuel penalties could be underestimated.

Study	**Region**	**Flight rerouting strategy**	**NWP data**	**Air traffic data**	**Number of flights**	**Flights rerouted**	**Fleet-wide fuel increase**	**Contrail mitigation potential**
[1]	Japan	vertical	reanalysis	flown trajectories	149000	1.7 %	0.014 %	59.3 %
[2]	North America	vertical & lateral*	forecasts	flight plans	84839	13 %	0.11 %	73 %
[3]	Central & Southern Europe	vertical & lateral*	forecasts & reanalysis	flown trajectories	25†	2–8 %†	0.14 %	56 %
this study	Northern Europe	vertical	reanalysis	flight plans	145092	9 %	0.37 %	48.2 %

Table 3. Overview for different contrail avoidance studies, including Teoh et al. (2020a) [1], Martin Frias et al. (2024) [2], Kirschler et al. (2026) [3]. † For the study by Kirschler et al. (2026) note that they conducted 25 actual contrail avoidance flights in a real world trial and subsequently estimated the fleet-wide impact based on their experimental findings, whereas all other studies (including this one) merely carried out simulations. * The studies by Martin Frias et al. (2024) and Kirschler et al. (2026) utilized commercial flight planning tools and considered airspace constraints.

Fig. 7f shows the mitigation potential against the relative change in fleet-wide fuel burn. The results indicate that 58.2 % of the possible total CO_2eq saving can be achieved without any changes in the fleet-wide fuel burn (again due to apparently non-fuel-optimal original flight plans). For 100 % mitigation potential, we estimate an increase of 0.37 % for the fleet-wide fuel burn.

https://doi.org/10.5194/jecats-2026-14
Preprint. Discussion started: 14 August 2026

Table 3 compares our results against other studies, all based on the same contrail model but covering different geographical domains, applying different trajectory rerouting strategies, using different weather and air traffic data, and consequently finding different impacts on the amount of flights rerouted, the fleet-wide fuel increase, and the contrail mitigation potential. Despite these differences, 3 out of 4 studies (including this one) show reasonable agreement, with approximately 10 % flights rerouted, a fleet-wide fuel increase of 0.1–0.4 % and a reduction of contrail climate effects by 50–70 %; thus, these results appear to be robust.

Fig. 7b shows the distribution against the ratios of standard error to mean total CO_2eq saving which we use to quantify the weather-dependent uncertainty in the modeling of the total CO_2eq saving. The definition of confidence interval CI for a normal distribution is

$$CI_{\text{upper/lower}} = \text{mean} \pm t \times \text{standard error}, \tag{2}$$

with t depending on the sample size and the confidence level (Henze, 2010). Thus, we can estimate that here (with the 10-member meteorology ensemble) the lower end of the 95 % two-sided confidence interval (thus, $t = 2.262$) of the potential saving is positive for ratios $< 44\,\%$, corresponding to 97.8 % of the achievable saving. In other words, even when conservatively confining to cases for which the climate benefit is positive with a chance of 97.5 %, the majority of the possible climate mitigation potential can be realized. A lower end of at least half of the mean (an even more conservative approach) is given for ratios $< 22\,\%$, allowing 87.2 % of the achievable saving. 60 % of the possible total CO_2eq saving can be achieved for ratios of standard error to mean total CO_2eq saving $\leq 11.7\,\%$. Consequently, significant parts of the mitigation potential can be achieved by focusing on economically acceptable additional fuel consumptions or high-certainty CO_2eq predictions.

Based on the full optimization we consider different subsets of climate-optimized flights, including optimization strategies selecting a) only the most relevant flights with respect to CO_2eq savings, b) flights based on the maximum allowed fuel burn increase (for single but complete flights), or c) flights based on the maximum allowed ratio of the 10-member meteorology ensemble standard error and the mean total CO_2eq saving. Figure 8 shows the results both for the ANSP and the AU perspective, with the latter being smaller due to the inclusion of unoptimized waypoints outside the Borealis alliance airspace. Focusing on the ANSP perspective, we find that trajectory adaptations mainly reduce the CO_2eq related to contrails, whereas changes in CO_2 and NO_x are negligible. The full optimization reduces the contrail impact by about 48.2 %; considering only one quarter of those flight optimizations allows for a 41.4 % reduction. Even adjusting only the 100 most impactful flights according to the contrail effect allows to reduce the latter by about 6.6 %. Confining the optimization to fuel burn increases $< 1\,\%$ leads to a 24.7 % reduction of contrail CO_2eq. Allowing larger fuel burn increases still increases the mitigation potential, but with decreasing efficiency. Results are in agreement with Fig. 7e (red curve as fuel burn changes are given for the full flight in Fig. 8). Also a limitation to uncertainties (relative standard error over mean for the 10-member meteorology ensemble) $< 10\,\%$ leads to a saving of 25.2 % contrail CO_2eq (again in agreement with Fig. 7b).

https://doi.org/10.5194/jecats-2026-14
Preprint. Discussion started: 14 August 2026

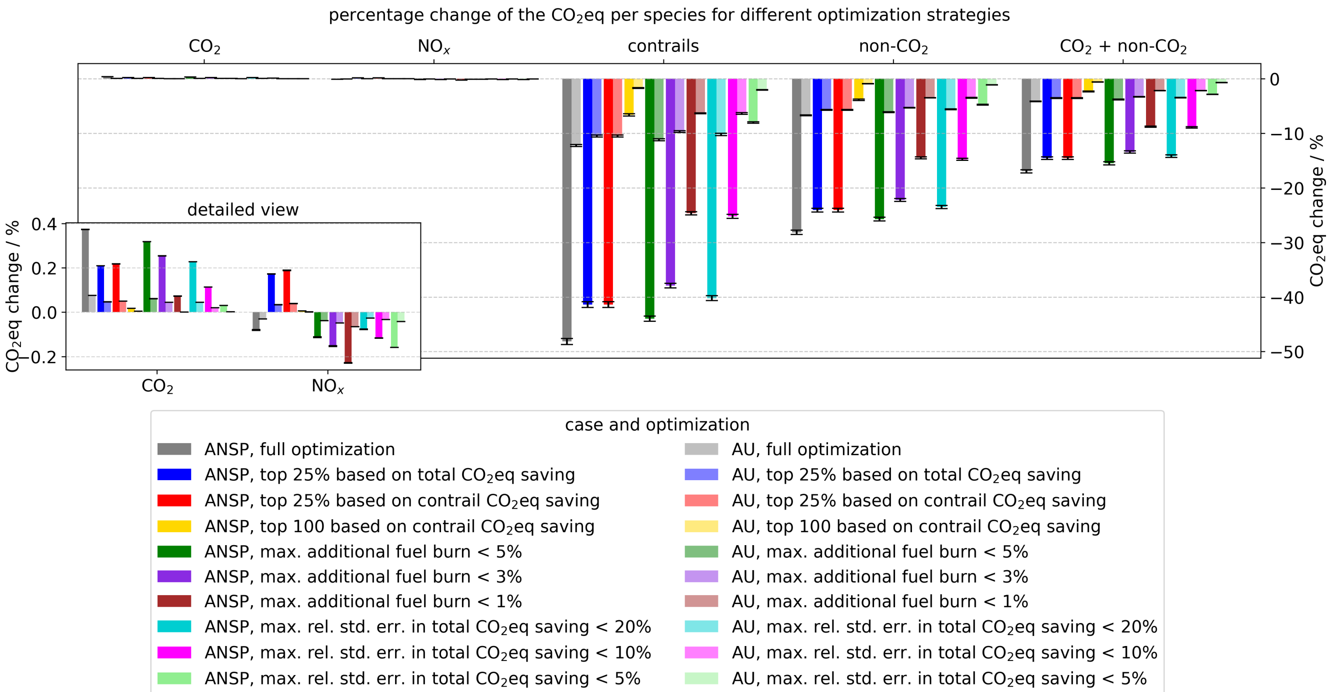

Figure 8. 10-member ensemble mean relative changes in CO_2eq per species for different air traffic optimization strategies. Results are given for ANSP-perspective including only waypoints within Borealis alliance airspace at the study dates (bold) and for AU-perspective including all waypoints of flights with at least one waypoint within the Borealis alliance airspace at the study dates (faint). The uncertainty range indicates the 95 % confidence interval of the mean based on the 10-member meteorology ensemble. A detailed representation of results for CO_2 and NO_x is shown in the inset, using a different y-axis due to the large difference in changes for CO_2 and NO_x compared to the situation for contrails.

3.2.2 Operational impact

To first order, the complexity of a climate optimization strategy for ANSPs/AUs increases with the amount of flights that are modified. Thus, the corresponding fractions per date and per day-/nighttime are given for the full flight optimization in Fig. 9, with flights categorized based on their mid-flight time and position. Based on the presence of sunlight, flights during night are more often optimized than during day, which reflects the fact that contrails always have a warming radiative effect in the absence of daylight (compare also, e.g., Fig. 9f of Teoh et al., 2024). As flight schedules are generally independent of daylight, we consider also a static differentiation of day (6-18 UTC) and night (18-6 UTC); the results are qualitatively similar.

3.5–13.6 % of the flights are optimized during daytime, but 5.6–17.2 % during nighttime. Again, the days with large climate effect in September and December stand out, requiring optimization of $> 10\,\%$ of all flights independent of the day- or nighttime. Although it was shown in Sec. 3.1.2 that only 6 % of all flights in the Borealis area cause 80 % of the total contrail CO_2eq, Fig. 9 demonstrates that these flights are not equally distributed, but that during contrail impact peaks about 3 times as

https://doi.org/10.5194/jecats-2026-14
Preprint. Discussion started: 14 August 2026

many flights (in relative terms) need to be rerouted. Note that as the Borealis alliance domain covers rather high latitudes, the number of daylight hours varies significantly stronger between seasons than at mid-latitudes; consequently, also the variability in Fig. 9 might be stronger than for, e.g., typical Central European air traffic.

Rerouting air traffic to avoid Eco-areas might result in increased air traffic densities in neighboring airspaces. To evaluate this, flight concentrations are counted based on a grid covering the Borealis alliance airspace with a resolution of 2°, the flight altitudes between 19500 ft and 41500 ft with 1000 ft resolution, and the 16 study days with a temporal resolution of 10 min. Considering typical cruise speeds of 900 $\mathrm{km\,h^{-1}}$, an aircraft passes 150 km in 10 min which approximately corresponds to 2° at 60° N; thus, aircraft are expected to have moved to different spatial grid cells and produce different density configurations for each timestep. The size of the described grid is assumed to be the overall available airspace and used to derive corresponding fractions. Figure 10 shows that in most cases only a single aircraft is located in a grid cell (corresponding to 2.5 % of the available 4-dimensional airspace), whereas high concentrations occur rarely. For example, concentrations of 4 (10) aircraft per grid cell are about 2 (4) orders of magnitude less frequent than a single aircraft per grid cell. Considering the fully optimized air traffic, the distribution is generally the same. However, the occurrence of 4–9 flights per grid cell is increased by about 3 %. Fig 11 shows the change in the amount of grid cells with 4–12 aircraft after full optimization for the different time periods, ANSP sectors and altitudes. Fig 11b indicates that such cases occur less often at altitudes of 32000 ft and higher (relative reductions up to 100 % per date and altitude) but more frequently at 30000 ft and 31000 ft (relative increases $> 100\,\%$). This demonstrates the expected behavior, with flights being rerouted to lower altitudes to avoid contrails, consequently forming a new hot spot region. Inspecting changes per ANSP sector leads to a mixed picture of increases and decreases in the occurrence of grid cells with 4–12 aircraft (Fig 11a). However, there are i) increases which are strong in relative ($> 100\,\%$) but small in absolute terms (e.g., Finland, EFIN, Estonia, EETT, Latvia, EVRR on 16–17 September), as well as cases ii) with small relative changes (10–15 %) but which are notable in absolute terms (ca. 70, see EGTT on 21–22 and 27-28 December).

For safety reasons, aircraft need to obey specific regulatory-required separations. For instance, a horizontal separation of 5 NM is necessary when air traffic control (ATC) has access to sufficient surveillance systems (with larger separations otherwise; see ICAO, 2016). Thus, we evaluate the horizontal distance to another flight for each trajectory waypoint (considering waypoints above 20000 ft and at even flight altitudes such as 20000 ft, 21000 ft, 22000 ft etc.) and select the minimum horizontal separation (MHS) for each pair of flights. Each pairing of flights is counted once. Results are shown in Fig. 12; note that the integral over the histogram does not need to be constant when changing altitudes of individual flights. Fig. 12 shows that MHS for the original air traffic peaks around 65 NM, although also separations ≤ 10 NM are often found; note that a calculation of MHS based on ADS-B data (i.e., actually flown trajectories; not shown) produces nearly no separations < 10 NM, indicating that such close encounters are solved tactically by ATC. Considering the fully optimized air traffic, all MHS occur more often (including ≤ 5 NM). In some cases the increase in MHS is even of similar order of magnitude as the fraction of rerouted flights (e.g., around 10 % for MHS of 5 NM). For comparison, in a modelling case study considering the Japanese airspace, Teoh et al. (2020b) derived a ratio of about 10 % between flights in conflict and rerouted flights, whereas Ehrmanntraut (2023) reported a capacity reduction of 20 % under moderate traffic conditions based on a real-time simulation for MUAC. In Fig. 13 the events with MHS ≤ 10 NM are shown again for different dates, ANSP sectors and altitudes. Figure 13b shows again the consequence

https://doi.org/10.5194/jecats-2026-14
Preprint. Discussion started: 14 August 2026

of the vertical rerouting: separations $\leq 10\,\mathrm{NM}$ happen more often at 30000 ft, 26000 ft, and 22000 ft (relative increases of $\gg 100\,\%$) but generally less often above. Changes in separation events $\leq 10\,\mathrm{NM}$ per ANSP sector are again very mixed, see Fig. 13a, with the same cases standing out as in Fig 11a: i) on 16–17 September, Finland (EFIN), Estonia (EETT), and Latvia (EVRR) experience > 20 additional events with MHS $\leq 10\,\mathrm{NM}$, which corresponds to an increase of more than $\gg 100\,\%$; ii) on 21–22 and 27–28 December, England (EGTT) experiences a relative change of ca. 20–30 % in events with separations $\leq 10\,\mathrm{NM}$ which, however, corresponds to far more than 100 cases per 48 h-period.

Overall, the operational impact remains inconclusive. On average over the full spatial and temporal domain, changes in concentrations and small horizontal separation events appear relatively small. Given that, e.g., critical separations occur already for the original planned flight trajectories–events that are tactically solvable by ATC–it appears feasible that the relatively small number of additional small horizontal separations could be solved as well. However, for specific days and ANSP sectors the absolute and/or relative increase in potentially critical events (either derived from flight pairs with MHS $< 10\,\mathrm{NM}$ or from the occurrence of concentrations with 4–12 aircraft per grid cell) are significant, potentially indicating a limitation of contrail avoidance maneuvers due to ATC.

3.3 Limitations

This study tries to follow as closely as possible the setup defined for the MRV. Still, some limitations of the quantitative outcome need to be taken into account:

- Not using the aCCF alignment to the more complex climate response model AirClim—i.e., using version 1.0 (Yin et al., 2023) instead of 1.0A (Simorgh et al., 2024), see Sec. 2.3.2—would generally increase the NO_x-induced climate effects reported here by about a factor 5 (O_3 increases by a factor 5.6, CH_4 plus PMO increases by a factor 17). aCCF version 1.0A was critically discussed, with raised issues including, e.g., the complex and potentially unclear derivation of the aCCFs from various models and simulations, the insufficient justification for the usage of AirClim as reference model, the unclear functional relation between results from aCCF and AirClim using tagging and perturbation approaches, respectively, an unconventional choice of climate metric, and the sheer size of the resulting alignment factors (see Anonymous Referee #2, 2024).

- GWP is used in this study, which is the mainly reported climate metric of the IPCC, although limitations, uncertainties and application-dependencies of the climate metric-choice are acknowledged and no conclusive recommendation has been made (Shukla et al., 2022; UNFCCC SBSTA, 2023). Considering an efficacy-weighted GWP instead of the unweighted GWP would decrease the contrail climate effect by a factor 0.42 (Lee et al., 2021), 0.37 (Borella et al., 2024) or 0.21 (Bickel et al., 2025), depending on the assumed globally averaged efficacy value. Regionally, the surface temperature response is distinctly non-homogeneous (Ponater et al., 2005) and is known to be determined by both the forcing and the feedback patterns (e.g., Boer and Yu, 2003; Juvin-Quarroz et al., 2026). Additionally, feedbacks may be expected to be case-specific for contrail cirrus (Juvin-Quarroz et al., 2026).

https://doi.org/10.5194/jecats-2026-14
Preprint. Discussion started: 14 August 2026

- This flight optimization study is based on reanalysis NWP data and, thus, represents an optimal case in the sense that there are no weather forecast uncertainties, but actual measurements were assimilated during the reanalysis process. However, reanalysis NWP data is of course not available for real operations. Usage of actual NWP forecasts would reduce the contrail mitigation potential on average by roughly 30 % for lead times of 48 h (Dean et al., 2025) due to inaccuracies in the prediction the ambient meteorology and particularly of ISSRs.

- The estimation of the 95 % confidence intervals are purely based on the meteorological variability in the reanalysis data, not on forecast data. Within the weather data, the most critical quantity is the predicted relative humidity: As stated in Sec. 2.2.1, a correction is applied to handle a known underestimation of the relative humidity by NWP models. As the contrail persistence and climate effect strongly depends on the ambient humidity, it has a significant impact on the CoCiP output. Teoh et al. (2022a) conducted CoCiP simulations with and without humidity correction, finding a 49 % smaller annual mean contrail radiative effect for the North Atlantic when not correcting the relative humidity. Similarly, Schumann et al. (2021b) reported that a change of $\pm 5\,\%$ in relative humidity changes the net contrail radiative effect by around 60 %. Despite corrections, the prediction of the relative humidity might be one of the most important sources for uncertainty when predicting contrails. Beyond NWP issues, also other model uncertainties are not taken into account, e.g., from CoCiP and aCCFs, due to the radiative effect parametrization, etc. Consequently, the results presented in this study are a lower bound on the confidence intervals.

- Flight trajectories are based on actual flight plans filed to NM before departure. Those flight plans do not reflect operational impacts. Directs offered in-flight by ATC might lower fuel burn and flight time, airspace limitations from severe weather etc. might increase them, whereas delayed departures might render pre-tactical climate optimizations ineffective.

4 Conclusions and outlook

Flight trajectories of the full air traffic crossing the Borealis alliance airspace (including Iceland, United Kingdom, Ireland, Scandinavia, part of the Baltics and the Northern Atlantic with large parts of the North Atlantic flight corridor) at 16 selected days in 2023 have been climate-optimized by applying vertical reroutings. Relevant flights and flight segments have been identified and optimized using a new concept called "Eco-areas", denoting 4D airspaces that are prone to producing a warming climate effect exceeding a certain, non-zero threshold. Different flight selections for the overall air traffic optimization have been explored. As a novelty, this study combines the climate response models CoCiP for contrails and aCCFs for NO_x (which is the modeling approach implemented in the EU's non-CO_2 MRV) to estimate the total CO_2eq based on the climate metric GWP100, including 95 % confidence intervals due to meteorological ensemble inputs. Based on these simulations, the following conclusions can be drawn:

- Regarding the annual average, the climate effect of CO_2 and non-CO_2 are about the same; the same holds for contrails and NO_x.

https://doi.org/10.5194/jecats-2026-14
Preprint. Discussion started: 14 August 2026

- Nearly half of climate effect due to contrails could be avoided by vertical trajectory optimizations. Around 40 % reduction is already achievable when limiting to additional fuel burns per rerouted flight $< 5\,\%$ and meteorological uncertainties $< 20\,\%$.
- Climate effects due to NO_x could not be significantly reduced in the presented approach, in particular as NO_x effects are much less localized than contrail effects.
- The contrail climate effect is temporally and spatially localized. During the studied time periods, no more than ca. 3 out of 11 ANSPs simultaneously experienced strong climate effects related to contrails (i.e., high total CO_2eq).
- About 6 % of all flights and less than 2 % of the total flight distance caused 80 % of the total cumulative contrail CO_2eq. However, these flights are temporally not homogenously distributed. During some time periods, about 17 % of the flights might require trajectory optimizations. Fortunately, the need for optimization peaks at night, i.e., during times with comparably lower air traffic.
- As expected, spatio-temporal flight concentrations are slightly increased, whereas small horizontal separations occur more frequently. On average, increases in congestion are small relative to the typical flight concentrations and separations that we found already for the original air traffic scenario. This indicates that operational impacts are generally no obstacle for the implementation of contrail avoidance strategies. However, significant increase of events with potentially critical horizontal separations/spatio-temporal concentrations occurred in specific cases, and it remains unclear whether these changes are solvable by ATC.

This work can be extended in multiple ways. Similar regional case studies should be carried out for other airspaces, focusing particularly on complicated high air traffic domains (e.g., Central Europe). More thorough investigations on the impact of airspace capacity should be carried out, taking realistic ANSP capabilities and sector capacities into account. To increase the simulation's realism and allow for a more thorough uncertainty management, the air traffic optimization should be based on historical weather forecast data, with the outcome being evaluated against reanalysis data. The dependence of the optimization success on criteria such as the applied forecast lead time or the accepted forecast uncertainty could be investigated. The concept of operations should be revised, including a) the flight selection concept via Eco-areas, b) pre-tactical communication possibilities from ANSPs/NM to AUs regarding suggestions for trajectory modifications to reduce climate effects, c) tactical communication pathways of AUs to ANSPs regarding their climate-optimization status, and d) de-conflicting and prioritization rules for multiple climate-optimized flights; in particular b–d might require adjustments of the regulatory framework by EUROCONTROL. Finally, based on the demonstrated theoretical feasibility of pre-tactical climate-optimization of air traffic, such mitigation strategies need further testing via real world trials at increasing scale.

https://doi.org/10.5194/jecats-2026-14
Preprint. Discussion started: 14 August 2026

Appendix A: Air traffic filters

Upon inspecting the historical flight plan data provided by EUROCONTROL it was found that it most likely contained duplicates. Besides clear duplicates, the dataset contained the same or very similar trajectories under different callsigns. Based on the callsign (and the derived 3-digit airline ICAO code), aircraft type, and start and end points, three filters were applied where duplicates were determined based on the following criteria:

1. airline ICAO code, start and end time (rounded to 60 minutes), first and last latitude and longitude (rounded to one decimal place)
2. aircraft type, start and end time (rounded to 10 minutes), first and last latitude and longitude (rounded to one decimal place)
3. callsign (first 6 letters), start and end time (rounded to 60 minutes)

Appendix B: Derivation of CO_2eq

The derivation of all CO_2eq combines CoCiP, CLIMaCCF and literature results. First, the absolute global warming potential (AGWP) for a time horizon of $H = 100$ years is derived from the model results for all forcers. Second, the global warming potential (GWP) is derived as the unitless ratio of $AGWP_{forcer}$ and $AGWP_{CO_2}$. Third, the CO_2eq mass is calculated by multiplying the GWP ratio with the emitted CO_2 mass. Note that efficacies are not considered. A pulse emission is assumed.

For contrails, $AGWP_{cont}$ per flight distance (in units of J m^{-2} m^{-1}) is derived as

$$AGWP_{cont} = \int_{t_0}^{t_0+H} RF_{cont}(t)dt \tag{B1}$$

$$\approx \int_{t_0}^{t_0+H} \frac{iRF_{cont}(t) \times W(t) \times L(t)}{S_{Earth}} dt \tag{B2}$$

$$= \frac{EF_{cont}}{S_{Earth}} \tag{B3}$$

with S_{Earth} denoting Earth's surface area, W and L being the contrail's width and length, RF_{cont} its radiative forcing, iRF_{cont} its instantaneous radiative forcing, and EF_{cont} its energy forcing (with the last three quantities per flight distance). As the RF_{cont} is a global mean, the ratio of the contrails horizontal extent and the Earth's surface is included. Using the iRF instead of RF is an approximation as stratospheric adjustments are neglected. Additionally, the iRF from CoCiP is rather a radiative effect than a radiative forcing as it is calculated relative to the contrail-free case, not pre-industrial conditions. As H is generally much larger than typical contrail lifetimes, the time integral can be replaced by the full EF predicted by CoCiP. Next, $AGWP_{cont}$ is divided by

$$AGWP_{CO_2} = 88.0 \times 10^{-15}\,\mathrm{W\,m^{-2}\,kg(CO_2)^{-1}yr} \tag{B4}$$

https://doi.org/10.5194/jecats-2026-14
Preprint. Discussion started: 14 August 2026

which is based on Gaillot et al. (2023). Note that the $AGWP_{CO2}$ by Gaillot et al. (2023) is close to the estimate of $92.5 \times 10^{-15}\,\mathrm{W\,m^{-2}\,kg(CO_2)^{-1} yr}$ by Joos et al. (2013). After a division by $EI_{CO_2} = 3.159$ and a multiplication with the flight distance per fuel burned as simulated with CoCiP, one arrives at a unitless ratio.

For gaseous emissions, CLIMaCCF outputs are converted from their native output pulse average temperature response for a 20 year horizon (P-ATR20) to pulse AGWP for a 100 year horizon (P-AGWP100) using corresponding conversion factors (see C). For O_3 and CH_4 results are given relative to the mass of NO_2 emitted and not per fuel burned; thus, corresponding values are multiplied by the NO_x emission per fuel mass, which is taken from flight segment-specific CoCiP simulations for trajectory calculations (internally using the Boeing fuel flow method 2 and the ICAO EDB, see also Sec. 2.3.1) or set to 0.01514 (Lee et al., 2021) for grid calculations. Instead of using $AGWP_{CO_2}$ from Gaillot et al. (2023) as for contrails, the estimate from CLIMaCCF calculations is considered to derive the GWP; thus, the gaseous non-CO_2 emissions are treated consistently in the sense that all AGWPs come from CLIMaCCF. However, $AGWP_{CO_2}$ from CLIMaCCF is circa 8 % smaller (see C) than the corresponding estimate by Gaillot et al. (2023), eventually leading to an increase in the estimates for the CO_2eq by the same percentage.

Finally, the emitted CO_2 mass is taken from flight segment-specific CoCiP simulations for trajectory calculations (internally using BADA3 and EI_{CO_2}, see also Sec. 2.3.1).

Appendix C: Conversion from P-ATR20 to P-AGWP100

Dahlmann et al. (2025) presented a set of constant, multiplicative conversion factors that allow to switch between different climate metrics. They give results for four emission scenarios, five climate metrics and four time horizons, based on calculations with the climate response model AirClim and the REACT4C emission inventory (see their paper for details). In this study, we apply conversion factors to turn the average temperature response over a 20 yr horizon for a pulse emission (P-ATR20, the native output of CLIMaCCF) into the corresponding absolute global warming potential for a 100 yr time horizon for the same emission scenario (P-AGWP100) (Table C1). We use an older, unpublished version of the conversion factors which follows the methodology of Dahlmann et al. (2025), but which was derived without efficacies and used the parameterization of Sausen and Schumann (2000) instead of the one by Boucher and Reddy (2008) for the surface temperature evolution depending on the radiative forcing.

Species	Conversion factor / $\mathrm{W\,m^{-2}\,K^{-1}\,yr}$
CO_2	343.03
H_2O	66.22
O_3	66.22
CH_4	116.38
PMO	116.38

Table C1. Conversion factors to derive P-AGWP100 from P-ATR20 values.

For example, the P-ATR20 value of CO_2 from Yin et al. (2023) is $7.48 \times 10^{-16}\,\mathrm{K\,kg(fuel)^{-1}}$; multiplied by the factor $343.03\,\mathrm{W\,m^{-2}\,K^{-1}\,yr}$ (see Table C1) and divided by $EI_{CO_2} = 3.159$ gives $81.2 \times 10^{-15}\,\mathrm{W\,m^{-2}\,kg(CO_2)^{-1}\,yr}$ which is smaller but of the same oder of magnitude as corresponding results of Joos et al. (2013) and Gaillot et al. (2023).

Appendix D: Seasonal cycle of NO_x effectiveness

Castino et al. (2021) reported a seasonal dependence of the NO_x climate effects per flight length when considering the climate metric ATR20 and the European air traffic. For NO_x and O_3, they found a maximum climate effect for the months August and September, and a minimum for February to April, whereas CH_4 exhibited an inverted behavior. A similar dependence is also visible in our results (see Fig. D1), with largest values for NO_x-related CO_2eq per flight distance for the study days in September, and lowest values in March and December.

Code and data availability. Code and data presented in this study are available upon request from the corresponding author.

Author contributions. Conceptualization, DP.; data curation, DP, KW, SK, JC, and JE; formal analysis, DP; funding acquisition, DA, SM, FY, and CV; investigation, DP, KW, JC, JE, and JS; methodology, DP, SD, SM, and KD; project administration, DP and DA; software, DP, KW, SK, JC, JE, and JS; supervision, FY and CV; validation, JC and JS; visualization, DP; writing - original draft, DP, KW, JS, and SD; writing - review & editing, DP, KW, SK, JC, JE, JS, DA, TP, SD, SM, KD, FY, and CV. All authors have read and agreed to the published version of the manuscript.

Competing interests. JC, JE, and DA are employed by Thales S.A. TP is employed by Integra Consult A/S. FY and SM are members of the editorial board of the Journal of Environmentally Compatible Air Transport System (JECATS). The other authors declare that they have no competing interests.

Acknowledgements. The authors acknowledge funding by SESAR program grant no 101114785 (CONCERTO). Meteorological data was provided by ECMWF (European Centre for Medium-Range Weather Forecasts). Base of Aircraft Data (BADA) version 3 and flight plan data has been made available by EUROCONTROL (European Organisation for the Safety of Air Navigation). The authors gratefully acknowledge the computational and data resources provided through the joint high-performance data analytics (HPDA) project "terrabyte" of the German Aerospace Center (DLR) and the Leibniz Supercomputing Center (LRZ).

References

Abrahamson, J. P., Zelina, J., Andac, M. G., and Vander Wal, R. L.: Predictive Model Development for Aviation Black Carbon Mass Emissions from Alternative and Conventional Fuels at Ground and Cruise, Environmental Science & Technology, 50, 12 048–12 055, https://doi.org/10.1021/acs.est.6b03749, 2016.

Aircraft Commerce (2005): Analysing the options for 757 replacement, Aircraft Commerce, 2005.

Aircraft Commerce (2018): A350-900/-1000 fuel burn operating performance, Aircraft Commerce, 2018.

Akhtar Martínez, C., Eastham, S. D., and Jarrett, J. P.: Zero-dimensional contrail models could underpredict lifetime optical depth, Atmospheric Chemistry and Physics, 25, 12 875–12 891, https://doi.org/10.5194/acp-25-12875-2025, 2025.

ALARM: Report on Algorithms for environmental (climate) hotspots, including MET data requirements for implementation, Tech. rep., Deutsches Zentrum für Luft- und Raumfahrt, 2022.

Andrews, S., Cathcart, J., Chen, A., Cornec, H., Kumar, S., Majholm, J., Meijers, M., Meijers, N., Miller, R., Mukhopadhaya, J., Sachdeva, N., Shapiro, M., Stern, C., and Wendling, Z. A.: Understanding Contrail Management: Opportunities, Challenges, and Insights, Tech. rep., Rocky Mountain Institute, 2024.

Anonymous Referee #2: Referee comment on "gmd-2023-92", https://doi.org/10.5194/gmd-2023-92-RC2, interactive comment on Geoscientific Model Development Discussions, 2024.

Arrowsmith, S., Lee, D. S., Owen, B., Faber, J., van Wijngaarden, L., Boucher, O., Celikel, A., Deransy, R., Fuglestvedt, J., Laukia, J., Tronstad Lund, M., Sausen, R., Schaefer, M., Skowron, A., Stromatas, S., and Watt, A.: Updated analysis of the non-CO2 climate impacts of aviation and potential policy measures pursuant to the EU Emissions Trading System Directive Article 30(4), Tech. rep., European Union Aviation Safety Agency, https://www.easa.europa.eu/en/document-library/research-reports/report-commission-european-parliament-and-council, 2020.

Baucom, I., Benham, E., Konijnenburg, J., Lee, G., Lippa, K., McGuire, J., Minnich, L., and Williams, J.: Specifications, Tolerances, and Other Technical Requirements for Weighing and Measuring Devices, Tech. rep., National Institute of Standards and Technology, https://doi.org/10.6028/NIST.HB.44-2026, 2026.

Bickel, M., Ponater, M., Burkhardt, U., Righi, M., Hendricks, J., and Jöckel, P.: Contrail Cirrus Climate Impact: From Radiative Forcing to Surface Temperature Change, Journal of Climate, 38, 1895 – 1912, https://doi.org/10.1175/JCLI-D-24-0245.1, 2025.

Boer, G. and Yu, B.: Climate sensitivity and response, Climate Dynamics, 20, 2003.

Borella, A., Boucher, O., Shine, K. P., Stettler, M., Tanaka, K., Teoh, R., and Bellouin, N.: The importance of an informed choice of CO2-equivalence metrics for contrail avoidance, Atmospheric Chemistry and Physics, 24, 9401–9417, https://doi.org/10.5194/acp-24-9401-2024, 2024.

Boucher, O. and Reddy, M.: Climate trade-off between black carbon and carbon dioxide emissions, Energy Policy, 36, 193–200, https://doi.org/10.1016/j.enpol.2007.08.039, 2008.

Bräuer, T., Voigt, C., Sauer, D., Kaufmann, S., Hahn, V., Scheibe, M., Schlager, H., Diskin, G. S., Nowak, J. B., DiGangi, J. P., Huber, F., Moore, R. H., and Anderson, B. E.: Airborne Measurements of Contrail Ice Properties—Dependence on Temperature and Humidity, Geophysical Research Letters, 48, e2020GL092 166, https://doi.org/10.1029/2020GL092166, 2021.

Burkhardt, U. and Kärcher, B.: Process-based simulation of contrail cirrus in a global climate model, Journal of Geophysical Research: Atmospheres, 114, https://doi.org/10.1029/2008JD011491, 2009.

https://doi.org/10.5194/jecats-2026-14
Preprint. Discussion started: 14 August 2026

Burkhardt, U. and Kärcher, B.: Global radiative forcing from contrail cirrus, Nature Climate Change, 1, 54–58, https://doi.org/10.1038/nclimate1068, 2011.

Castino, F., Yin, F., Grewe, V., Yamashita, H., Matthes, S., Baumann, S., Dietmüller, S., Soler, M., Simorgh, A., Linke, F., and Lührs, B.: Seasonal Variability of Aircraft Trajectories reducing NOx-climate Impacts under a Multitude of Weather Patterns, in: 11th SESAR Innovation Days, 2021.

Castino, F., Yin, F., Grewe, V., Yamashita, H., Matthes, S., Dietmüller, S., Baumann, S., Soler, M., Simorgh, A., Mendiguchia Meuser, M., Linke, F., and Lührs, B.: Decision-making strategies implemented in SolFinder 1.0 to identify eco-efficient aircraft trajectories: application study in AirTraf 3.0, Geoscientific Model Development, 17, 4031–4052, https://doi.org/10.5194/gmd-17-4031-2024, 2024.

Cohen, Y., Hauglustaine, D., Staniaszek, Z., Lund, M. T., Dedoussi, I., Matthes, S., Quadros, F., Righi, M., Skowron, A., and Thor, R.: Impact of present aircraft NO_x and aerosol emissions on atmospheric composition and climate: results from a model intercomparison, EGUsphere, 2025, 1–43, https://doi.org/10.5194/egusphere-2025-4273, 2025.

Dahlmann, K., Matthes, S., and Grewe, V.: Conversion of climate metrics for policy applications, https://doi.org/10.5281/zenodo.16355781, 2025.

Dameris, M., Grewe, V., Köhler, I., Sausen, R., Brühl, C., Grooß, J.-U., and Steil, B.: Impact of aircraft NOx emissions on tropospheric and stratospheric ozone. part II: 3-D model results, Atmospheric Environment, 32, 3185–3199, https://doi.org/10.1016/S1352-2310(97)00505-0, 1998.

Dean, T. R., Abbott, T. H., Engberg, Z., Masson, N., Teoh, R., Itcovitz, J. P., Stettler, M. E. J., and Shapiro, M. L.: Impact of forecast stability on navigational contrail avoidance, https://doi.org/10.1088/2634-4505/ae1da5, 2025.

Dickson, N., Gierens, K., Rogers, H., and Jones, R.: Vertical spatial scales of ice supersaturation and probability of ice supersaturated layers in low resolution profiles of relative humidity, in: TAC-2 Proceedings, June 22nd to 25th, 2009, Aachen and Maastricht, 2009.

Dietmüller, S., Matthes, S., Dahlmann, K., Yamashita, H., Simorgh, A., Soler, M., Linke, F., Lührs, B., Meuser, M. M., Weder, C., Grewe, V., Yin, F., and Castino, F.: A Python library for computing individual and merged non-CO_2 algorithmic climate change functions: CLIMaCCF V1.0, Geoscientific Model Development, 16, 4405–4425, https://doi.org/10.5194/gmd-16-4405-2023, 2023.

Dischl, R., Kaufmann, S., and Voigt, C.: Regional and Seasonal Dependence of the Potential Contrail Cover and the Potential Contrail Cirrus Cover over Europe, Aerospace, 9, https://doi.org/10.3390/aerospace9090485, 2022.

Dischl, R., Sauer, D., Voigt, C., Harlaß, T., Sakellariou, F., Märkl, R., Schumann, U., Scheibe, M., Kaufmann, S., Roiger, A., Dörnbrack, A., Renard, C., Gauthier, M., Swann, P., Madden, P., Luff, D., Johnson, M., Ahrens, D., Sallinen, R., Schripp, T., Eckel, G., Bauder, U., and Le Clercq, P.: Measurements of particle emissions of an A350-941 burning 100 % sustainable aviation fuels in cruise, Atmospheric Chemistry and Physics, 24, 11 255–11 273, https://doi.org/10.5194/acp-24-11255-2024, 2024.

Ehrmanntraut, R.: Contrail Prevention: MUAC Real Time Simulations April 2023, Tech. rep., Maastricht Upper Area Control Centre, 2023.

Ehrmanntraut, R.: COAV Project: MUAC Report on 100-Flights Contrail Trial 2024, Tech. rep., Maastricht Upper Area Control Centre, 2025.

Eichinger, R., Dahlmann, K., Grewe, V., Matthes, S., Niklaß, M., Lau, A., Zengerling, Z., Dietmüller, S., Völk, S., Megill, L., Voigt, C., Piontek, D., Kirschler, S., Plohr, M., Beckmann, B.-R., Schlemmer, L., Hanst, M., Hollborn, S., Seifert, A., and Fundel, F.: Reference set of technical specifications for the MRV, Tech. rep., Deutsches Zentrum für Luft- und Raumfahrt, Deutscher Wetterdienst, 2025.

Engberg, Z., Teoh, R., Abbott, T., Dean, T., Stettler, M. E. J., and Shapiro, M. L.: Forecasting contrail climate forcing for flight planning and air traffic management applications: the CocipGrid model in pycontrails 0.51.0, Geoscientific Model Development, 18, 253–286, https://doi.org/10.5194/gmd-18-253-2025, 2025.

https://doi.org/10.5194/jecats-2026-14
Preprint. Discussion started: 14 August 2026

EU Directive 2023/958: Directive (EU) 2023/958 of the European Parliament and of the Council of 10 May 2023 amending Directive 2003/87/EC as regards aviation's contribution to the Union's economy-wide emission reduction target and the appropriate implementation of a global market-based measure, Official Journal of the European Union, L 130, pp. 115–133, http://data.europa.eu/eli/dir/2023/958/oj, 2023.

EUROCONTROL: Study into the impact of the global economic crisis on airframe utilisation, EUROCONTROL, https://web.archive.org/web/20170221110344/https://www.eurocontrol.int/sites/default/files/content/documents/official-documents/facts-and-figures/coda-reports/study-impact-global-economic-crisis-2011.pdf, 2011.

EUROCONTROL: User Manual for the Base of Aircraft Data (BADA) Revision 3.16, EIH Technical/Scientific Report No. 22/05/12-45, EUROCONTROL Experimental Centre (EEC), https://www.eurocontrol.int/model/bada, 2022.

Freeman, S., Lee, D. S., Lim, L. L., Skowron, A., and De León, R. R.: Trading off Aircraft Fuel Burn and NO_x Emissions for Optimal Climate Policy, Environmental Science & Technology, 52, 2498–2505, https://doi.org/10.1021/acs.est.7b05719, 2018.

Frömming, C., Grewe, V., Brinkop, S., Jöckel, P., Haslerud, A. S., Rosanka, S., van Manen, J., and Matthes, S.: Influence of weather situation on non-CO2 aviation climate effects: the REACT4C climate change functions, Atmospheric Chemistry and Physics, 21, 9151–9172, https://doi.org/10.5194/acp-21-9151-2021, 2021.

Gaillot, T., Beauchet, S., Lorne, D., and Krim, L.: The impact of fossil jet fuel emissions at altitude on climate change: A life cycle assessment study of a long-haul flight at different time horizons, Atmospheric Environment, 311, 119 983, https://doi.org/10.1016/j.atmosenv.2023.119983, 2023.

Gierens, K.: The utility of partial contrail avoidance, Meteorologische Zeitschrift, 7, https://doi.org/10.1127/metz/1275, 2025.

Gierens, K. and Spichtinger, P.: On the size distribution of ice-supersaturated regions in the upper troposphere and lowermost stratosphere, Annales Geophysicae, 18, 499–504, https://doi.org/10.1007/s00585-000-0499-7, 2000.

Gierens, K., Matthes, S., and Rohs, S.: How Well Can Persistent Contrails Be Predicted?, Aerospace, 7, https://doi.org/10.3390/aerospace7120169, 2020.

Grewe, V., Frömming, C., Matthes, S., Brinkop, S., Ponater, M., Dietmüller, S., Jöckel, P., Garny, H., Tsati, E., Dahlmann, K., Søvde, O. A., Fuglestvedt, J., Berntsen, T. K., Shine, K. P., Irvine, E. A., Champougny, T., and Hullah, P.: Aircraft routing with minimal climate impact: the REACT4C climate cost function modelling approach (V1.0), Geoscientific Model Development, 7, 175–201, https://doi.org/10.5194/gmd-7-175-2014, 2014.

Harlass, T., Dischl, R., Kaufmann, S., Märkl, R., Sauer, D., Scheibe, M., Stock, P., Bräuer, T., Dörnbrack, A., Roiger, A., Schlager, H., Schumann, U., Pühl, M., Schripp, T., Grein, T., Bondorf, L., Renard, C., Gauthier, M., Johnson, M., Luff, D., Madden, P., Swann, P., Ahrens, D., Sallinen, R., and Voigt, C.: Measurement report: In-flight and ground-based measurements of nitrogen oxide emissions from latest-generation jet engines and 100 % sustainable aviation fuel, Atmospheric Chemistry and Physics, 24, 11 807–11 822, https://doi.org/10.5194/acp-24-11807-2024, 2024.

Henze, N.: Stochastik für Einsteiger, Vieweg + Teubner, Wiesbaden, Germany, ISBN 978-3-8348-0815-8, 2010.

Hersbach, H., Bell, B., Berrisford, P., Hirahara, S., Horányi, A., Muñoz-Sabater, J., Nicolas, J., Peubey, C., Radu, R., Schepers, D., Simmons, A., Soci, C., Abdalla, S., Abellan, X., Balsamo, G., Bechtold, P., Biavati, G., Bidlot, J., Bonavita, M., De Chiara, G., Dahlgren, P., Dee, D., Diamantakis, M., Dragani, R., Flemming, J., Forbes, R., Fuentes, M., Geer, A., Haimberger, L., Healy, S., Hogan, R. J., Hólm, E., Janisková, M., Keeley, S., Laloyaux, P., Lopez, P., Lupu, C., Radnoti, G., de Rosnay, P., Rozum, I., Vamborg, F., Villaume, S., and Thépaut, J.-N.: The ERA5 global reanalysis, Quarterly Journal of the Royal Meteorological Society, 146, 1999–2049, https://doi.org/10.1002/qj.3803, 2020.

https://doi.org/10.5194/jecats-2026-14
Preprint. Discussion started: 14 August 2026

Holzäpfel, F.: Probabilistic Two-Phase Wake Vortex Decay and Transport Model, Journal of Aircraft, 40, 323–331, https://doi.org/10.2514/2.3096, 2003.

ICAO, 2016: Doc 4444, Procedures for Air Navigation Services — Air Traffic Management, Sixteenth Edition, International Civil Aviation Organization, 2016.

ICAO, 2024: Annex 2 to the Convention on International Civil Aviation: Rules of the Air, International Civil Aviation Organization, 2024.

Joos, F., Roth, R., Fuglestvedt, J. S., Peters, G. P., Enting, I. G., von Bloh, W., Brovkin, V., Burke, E. J., Eby, M., Edwards, N. R., Friedrich, T., Frölicher, T. L., Halloran, P. R., Holden, P. B., Jones, C., Kleinen, T., Mackenzie, F. T., Matsumoto, K., Meinshausen, M., Plattner, G.-K., Reisinger, A., Segschneider, J., Shaffer, G., Steinacher, M., Strassmann, K., Tanaka, K., Timmermann, A., and Weaver, A. J.: Carbon dioxide and climate impulse response functions for the computation of greenhouse gas metrics: a multi-model analysis, Atmospheric Chemistry and Physics, 13, 2793–2825, https://doi.org/10.5194/acp-13-2793-2013, 2013.

Juvin-Quarroz, J., Borella, A., Kiepas, P., Dubos, T., Boucher, O., and Bellouin, N.: Atmospheric Adjustments to In Situ Cirrus Formation in Ice Supersaturated Regions, Journal of Geophysical Research: Atmospheres, 131, e2025JD046 235, https://doi.org/10.1029/2025JD046235, 2026.

Kaufmann, S., Dischl, R., and Voigt, C.: Regional and seasonal impact of hydrogen propulsion systems on potential contrail cirrus cover, Atmospheric Environment: X, 24, 100 298, https://doi.org/10.1016/j.aeaoa.2024.100298, 2024.

Kirschler, S., Voigt, C., Piontek, D., Juchem, M., Widmaier, K., Wang, Z., Nalianda, D., Todt, C., Zengerling, Z., Solzer, J., Lau, A., Schumann, U., Bellouin, N., Stettler, M., and Teoh, R.: Towards climate compatible aviation: operational feasibility of contrail avoidance by flight path adjustments, Research Square [preprint], https://doi.org/10.21203/rs.3.rs-8799231/v1, 2026.

Kärcher, B.: Formation and radiative forcing of contrail cirrus, Nature Communications, 9, https://doi.org/10.1038/s41467-018-04068-0, 2018.

Lee, D., Fahey, D., Skowron, A., Allen, M., Burkhardt, U., Chen, Q., Doherty, S., Freeman, S., Forster, P., Fuglestvedt, J., Gettelman, A., De León, R., Lim, L., Lund, M., Millar, R., Owen, B., Penner, J., Pitari, G., Prather, M., Sausen, R., and Wilcox, L.: The contribution of global aviation to anthropogenic climate forcing for 2000 to 2018, Atmospheric Environment, 244, 117 834, https://doi.org/10.1016/j.atmosenv.2020.117834, 2021.

Lewellen, D. C.: Persistent Contrails and Contrail Cirrus. Part II: Full Lifetime Behavior, Journal of the Atmospheric Sciences, 71, 4420 – 4438, https://doi.org/10.1175/JAS-D-13-0317.1, 2014.

Lewellen, D. C., Meza, O., and Huebsch, W. W.: Persistent Contrails and Contrail Cirrus. Part I: Large-Eddy Simulations from Inception to Demise, Journal of the Atmospheric Sciences, 71, 4399 – 4419, https://doi.org/10.1175/JAS-D-13-0316.1, 2014.

Lührs, B., Linke, F., Matthes, S., Grewe, V., and Yin, F.: Climate Impact Mitigation Potential of European Air Traffic in a Weather Situation with Strong Contrail Formation, Aerospace, 8, https://doi.org/10.3390/aerospace8020050, 2021.

Majka, A. and Pasich, A.: Cross-border Free Route Airspace concept and its impact on flight efficiency improvement, IOP Conference Series: Materials Science and Engineering, 1226, 012 022, https://doi.org/10.1088/1757-899X/1226/1/012022, 2022.

Mannstein, H., Spichtinger, P., and Gierens, K.: A note on how to avoid contrail cirrus, Transportation Research Part D: Transport and Environment, 10, 421–426, https://doi.org/10.1016/j.trd.2005.04.012, 2005.

Märkl, R. S., Voigt, C., Sauer, D., Dischl, R. K., Kaufmann, S., Harlaß, T., Hahn, V., Roiger, A., Weiß-Rehm, C., Burkhardt, U., Schumann, U., Marsing, A., Scheibe, M., Dörnbrack, A., Renard, C., Gauthier, M., Swann, P., Madden, P., Luff, D., Sallinen, R., Schripp, T., and Le Clercq, P.: Powering aircraft with 100 % sustainable aviation fuel reduces ice crystals in contrails, Atmospheric Chemistry and Physics, 24, 3813–3837, https://doi.org/10.5194/acp-24-3813-2024, 2024.

https://doi.org/10.5194/jecats-2026-14
Preprint. Discussion started: 14 August 2026

Martin Frias, A., Shapiro, M. L., Engberg, Z., Zopp, R., Soler, M., and Stettler, M. E. J.: Feasibility of contrail avoidance in a commercial flight planning system: an operational analysis, Environmental Research: Infrastructure and Sustainability, 4, 015 013, https://doi.org/10.1088/2634-4505/ad310c, 2024.

Matthes, S., Lim, L., Burkhardt, U., Dahlmann, K., Dietmüller, S., Grewe, V., Haslerud, A. S., Hendricks, J., Owen, B., Pitari, G., Righi, M., and Skowron, A.: Mitigation of Non-CO2 Aviation's Climate Impact by Changing Cruise Altitudes, Aerospace, 8, https://doi.org/10.3390/aerospace8020036, 2021.

Mayer, B. and Kylling, A.: Technical note: The libRadtran software package for radiative transfer calculations - description and examples of use, Atmospheric Chemistry and Physics, 5, 1855–1877, https://doi.org/10.5194/acp-5-1855-2005, 2005.

Megill, L., Deck, K., and Grewe, V.: Alternative climate metrics to the Global Warming Potential are more suitable for assessing aviation non-CO effects, Communications Earth & Environment, 5, 249, https://doi.org/10.1038/s43247-024-01423-6, 2024.

Molloy, J., Teoh, R., Harty, S., Koudis, G., Schumann, U., Poll, I., and Stettler, M. E. J.: Design Principles for a Contrail-Minimizing Trial in the North Atlantic, Aerospace, 9, https://doi.org/10.3390/aerospace9070375, 2022.

Niklaß, M., Lührs, B., Grewe, V., Dahlmann, K., Luchkova, T., Linke, F., and Gollnick, V.: Potential to reduce the climate impact of aviation by climate restricted airspaces, Transport Policy, 83, 102–110, https://doi.org/10.1016/j.tranpol.2016.12.010, 2019.

Penner, J., Lister, D., Griggs, D., Dokken, D., and McFarland, M., eds.: Aviation and the Global Atmosphere, Cambridge University Press, Cambridge, UK, https://archive.ipcc.ch/ipccreports/sres/aviation/index.php?idp=0, 1999.

Petzold, A., Khan, N. F., Li, Y., Spichtinger, P., Rohs, S., Crewell, S., Wahner, A., and Krämer, M.: Most Long-Lived Contrails Form within Cirrus Clouds with Uncertain Climate Impact, Nature Communications, 16, 9695, https://doi.org/10.1038/s41467-025-65532-2, 2025.

Poll, D. and Schumann, U.: An estimation method for the fuel burn and other performance characteristics of civil transport aircraft during cruise: part 2, determining the aircraft's characteristic parameters, The Aeronautical Journal, 125, 296–340, https://doi.org/10.1017/aer.2020.124, 2021.

Ponater, M., Marquart, S., Sausen, R., and Schumann, U.: On contrail climate sensitivity, Geophysical Research Letters, 32, https://doi.org/10.1029/2005GL022580, 2005.

Prather, M., Gettelman, A., and Penner, J.: Trade-offs in aviation impacts on climate favour non-CO2 mitigation, Nature, 643, 988–993, https://doi.org/10.1038/s41586-025-09198-2, 2025.

Quadros, F. D. A., Snellen, M., Sun, J., and Dedoussi, I. C.: Global Civil Aviation Emissions Estimates for 2017–2020 Using ADS-B Data, Journal of Aircraft, 59, 1394–1405, https://doi.org/10.2514/1.C036763, 2022.

Rosenow, J., Fricke, H., Luchkova, T., and Schultz, M.: Minimizing contrail formation by rerouting around dynamic ice-supersaturated regions, Aeronautics and Aerospace Open Access Journal, 3, 105–111, https://doi.org/10.15406/aaoaj.2018.02.00039, 2018.

Sausen, R. and Schumann, U.: Estimates of the Climate Response to Aircraft CO2 and NOx Emissions Scenarios, Climatic Change, pp. 27–58, https://doi.org/10.1023/A:1005579306109, 2000.

Sausen, R., Hofer, S., Gierens, K., Bugliaro, L., Ehrmanntraut, R., Sitova, I., Walczak, K., Burridge-Diesing, A., Bowman, M., and Miller, N.: Can we successfully avoid persistent contrails by small altitude adjustments of flights in the real world?, Meteorologische Zeitschrift, 33, 83–98, https://doi.org/10.1127/metz/2023/1157, 2024.

Schumann, U.: On conditions for contrail formation from aircraft exhausts, Meteorologische Zeitschrift, 5, 4–23, https://doi.org/10.1127/metz/5/1996/4, 1996.

Schumann, U.: A contrail cirrus prediction model, Geoscientific Model Development, 5, 543–580, https://doi.org/10.5194/gmd-5-543-2012, 2012.

https://doi.org/10.5194/jecats-2026-14
Preprint. Discussion started: 14 August 2026

Schumann, U. and Graf, K.: Aviation-induced cirrus and radiation changes at diurnal timescales, Journal of Geophysical Research: Atmospheres, 118, 2404–2421, https://doi.org/10.1002/jgrd.50184, 2013.

Schumann, U. and Heymsfield, A. J.: On the Life Cycle of Individual Contrails and Contrail Cirrus, Meteorological Monographs, 58, 3.1 – 3.24, https://doi.org/10.1175/AMSMONOGRAPHS-D-16-0005.1, 2017.

Schumann, U., Mayer, B., Graf, K., and Mannstein, H.: A Parametric Radiative Forcing Model for Contrail Cirrus, Journal of Applied Meteorology and Climatology, 51, 1391 – 1406, https://doi.org/10.1175/JAMC-D-11-0242.1, 2012.

Schumann, U., Hempel, R., Flentje, H., Garhammer, M., Graf, K., Kox, S., Lösslein, H., and Mayer, B.: Contrail study with ground-based cameras, Atmospheric Measurement Techniques, 6, 3597–3612, https://doi.org/10.5194/amt-6-3597-2013, 2013.

Schumann, U., Penner, J. E., Chen, Y., Zhou, C., and Graf, K.: Dehydration effects from contrails in a coupled contrail–climate model, Atmospheric Chemistry and Physics, 15, 11 179–11 199, https://doi.org/10.5194/acp-15-11179-2015, 2015.

Schumann, U., Baumann, R., Baumgardner, D., Bedka, S. T., Duda, D. P., Freudenthaler, V., Gayet, J.-F., Heymsfield, A. J., Minnis, P., Quante, M., Raschke, E., Schlager, H., Vázquez-Navarro, M., Voigt, C., and Wang, Z.: Properties of individual contrails: a compilation of observations and some comparisons, Atmospheric Chemistry and Physics, 17, 403–438, https://doi.org/10.5194/acp-17-403-2017, 2017.

Schumann, U., Bugliaro, L., Dörnbrack, A., Baumann, R., and Voigt, C.: Aviation Contrail Cirrus and Radiative Forcing Over Europe During 6 Months of COVID-19, Geophysical Research Letters, 48, e2021GL092 771, https://doi.org/10.1029/2021GL092771, e2021GL092771 2021GL092771, 2021a.

Schumann, U., Poll, I., Teoh, R., Koelle, R., Spinielli, E., Molloy, J., Koudis, G. S., Baumann, R., Bugliaro, L., Stettler, M., and Voigt, C.: Air traffic and contrail changes over Europe during COVID-19: a model study, Atmospheric Chemistry and Physics, 21, 7429–7450, https://doi.org/10.5194/acp-21-7429-2021, 2021b.

Seelig, T., Wolf, K., Bellouin, N., and Tesche, M.: Quantification of the Radiative Forcing of Contrails Embedded in Cirrus Clouds, Nature Communications, 16, 10 703, https://doi.org/10.1038/s41467-025-66231-8, 2025.

Shapiro, M., Engberg, Z., Teoh, R., Stettler, M., and Dean, T.: pycontrails: Python library for modeling aviation climate impacts, https://doi.org/10.5281/zenodo.10182539, 2023.

Shukla, P. R., Skea, J., Slade, R., Al Khourdajie, A., Hasija, A., Malley, J., Fradera, R., Belkacemi, M., Lisboa, G., McCollum, D., Vyas, P., Pathak, M., van Diemen, R., Luz, S., and Some, S., eds.: Climate Change 2022 - Mitigation of Climate Change: Working Group III Contribution to the Sixth Assessment Report of the Intergovernmental Panel on Climate Change, Cambridge University Press, https://doi.org/10.1017/9781009157926, 2022.

Simorgh, A., Soler, M., González-Arribas, D., Linke, F., Lührs, B., Meuser, M. M., Dietmüller, S., Matthes, S., Yamashita, H., and Yin, F.: Robust 4D Climate Optimal Flight Planning in Structured Airspace using Parallelized Simulation on GPUs: ROOST V1. 0, EGUsphere, 2022, 1–39, https://doi.org/10.5194/egusphere-2022-1010, publisher: Copernicus Publications Göttingen, Germany, 2022.

Simorgh, A., Soler, M., Dietmüller, S., Yamashita, H., and Matthes, S.: CLIMaCCF Library: database.py (line 23), https://github.com/dlr-pa/climaccf/blob/6d5696a42b8dbe32dc12f20ad585d12e2e149f97/climaccf/database.py#L23, gitHub repository, commit 6d5696a, 2024.

Smith, J. R., Grobler, C., Hodgson, P. J., Mukhopadhaya, J., Shapiro, M. L., Mirolo, M., Stettler, M. E. J., Eastham, S. D., and Barrett, S. R. H.: The climate opportunities and risks of contrail avoidance, Nature Communications, 17, 2092, https://doi.org/10.1038/s41467-026-68784-8, 2026.

Sonabend-W, A., Elkin, C., Dean, T., Dudley, J., Ali, N., Blickstein, J., Brand, E., Broshears, B., Chen, S., Engberg, Z., Galyen, M., Geraedts, S., Goyal, N., Grenham, R., Hager, U., Hecker, D., Jany, M., McCloskey, K., Ng, J., Norris, B., Opel, F., Rothenberg, J., Sankar, T.,

https://doi.org/10.5194/jecats-2026-14
Preprint. Discussion started: 14 August 2026

Sanekommu, D., Sarna, A., Schütt, O., Shapiro, M., Soh, R., Van Arsdale, C., and Platt, J. C.: Feasibility test of per-flight contrail avoidance in commercial aviation, Communications Engineering, 3, 184, https://doi.org/10.1038/s44172-024-00329-7, 2024.

Spichtinger, P., Gierens, K., Leiterer, U., and Dier, H.: Ice supersaturation in the tropopause region over Lindenberg, Germany, Meteorologische Zeitschrift, 12, 143–156, https://doi.org/10.1127/0941-2948/2003/0012-0143, 2003.

Stettler, M. E. J., Boies, A. M., Petzold, A., and Barrett, S. R. H.: Global Civil Aviation Black Carbon Emissions, Environmental Science & Technology, 47, 10 397–10 404, https://doi.org/10.1021/es401356v, pMID: 23844612, 2013.

Teoh, R., Schumann, U., Majumdar, A., and Stettler, M. E. J.: Mitigating the Climate Forcing of Aircraft Contrails by Small-Scale Diversions and Technology Adoption, Environmental Science & Technology, 54, 2941–2950, https://doi.org/10.1021/acs.est.9b05608, 2020a.

Teoh, R., Schumann, U., and Stettler, M. E. J.: Beyond Contrail Avoidance: Efficacy of Flight Altitude Changes to Minimise Contrail Climate Forcing, Aerospace, 7, https://doi.org/10.3390/aerospace7090121, 2020b.

Teoh, R., Schumann, U., Gryspeerdt, E., Shapiro, M., Molloy, J., Koudis, G., Voigt, C., and Stettler, M. E. J.: Aviation contrail climate effects in the North Atlantic from 2016 to 2021, Atmospheric Chemistry and Physics, 22, 10 919–10 935, https://doi.org/10.5194/acp-22-10919-2022, 2022a.

Teoh, R., Schumann, U., Voigt, C., Schripp, T., Shapiro, M., Engberg, Z., Molloy, J., Koudis, G., and Stettler, M. E. J.: Targeted Use of Sustainable Aviation Fuel to Maximize Climate Benefits, Environmental Science & Technology, 56, 17 246–17 255, https://doi.org/10.1021/acs.est.2c05781, 2022b.

Teoh, R., Engberg, Z., Schumann, U., Voigt, C., Shapiro, M., Rohs, S., and Stettler, M. E. J.: Global aviation contrail climate effects from 2019 to 2021, Atmospheric Chemistry and Physics, 24, 6071–6093, https://doi.org/10.5194/acp-24-6071-2024, 2024.

UNFCCC SBSTA: In-session technical workshop on findings on emission metrics contained in the Sixth Assessment Report of the Intergovernmental Panel on Climate Change, Tech. Rep. FCCC/SBSTA/2023/INF.2, United Nations Framework Convention on Climate Change (UNFCCC), Subsidiary Body for Scientific and Technological Advice (SBSTA), https://unfccc.int/documents/630115, Technical report by the Secretariat, 2023.

Unterstrasser, S., Gierens, K., Sölch, I., and Lainer, M.: Numerical simulations of homogeneously nucleated natural cirrus and contrail-cirrus. Part 1: How different are they?, Meteorologische Zeitschrift, 26, 621–642, https://doi.org/10.1127/metz/2016/0777, 2017a.

Unterstrasser, S., Gierens, K., Sölch, I., and Wirth, M.: Numerical simulations of homogeneously nucleated natural cirrus and contrail-cirrus. Part 2: Interaction on local scale, Meteorologische Zeitschrift, 26, 643–661, https://doi.org/10.1127/metz/2016/0780, 2017b.

van Manen, J. and Grewe, V.: Algorithmic climate change functions for the use in eco-efficient flight planning, Transportation Research Part D: Transport and Environment, 67, 388–405, https://doi.org/10.1016/j.trd.2018.12.016, 2019.

Vázquez-Navarro, M., Mannstein, H., and Kox, S.: Contrail life cycle and properties from 1 year of MSG/SEVIRI rapid-scan images, Atmospheric Chemistry and Physics, 15, 8739–8749, https://doi.org/10.5194/acp-15-8739-2015, 2015.

Voigt, C.: Solving aviation's climate-action conundrum, Nature, 643, 921–923, 2025.

Voigt, C., Schumann, U., Jurkat, T., Schäuble, D., Schlager, H., Petzold, A., Gayet, J.-F., Krämer, M., Schneider, J., Borrmann, S., Schmale, J., Jessberger, P., Hamburger, T., Lichtenstern, M., Scheibe, M., Gourbeyre, C., Meyer, J., Kübbeler, M., Frey, W., Kalesse, H., Butler, T., Lawrence, M. G., Holzäpfel, F., Arnold, F., Wendisch, M., Döpelheuer, A., Gottschaldt, K., Baumann, R., Zöger, M., Sölch, I., Rautenhaus, M., and Dörnbrack, A.: In-situ observations of young contrails – overview and selected results from the CONCERT campaign, Atmospheric Chemistry and Physics, 10, 9039–9056, https://doi.org/10.5194/acp-10-9039-2010, 2010.

Voigt, C., Lelieveld, J., Schlager, H., Schneider, J., Curtius, J., Meerkötter, R., Sauer, D., Bugliaro, L., Bohn, B., Crowley, J. N., Erbertseder, T., Groß, S., Hahn, V., Li, Q., Mertens, M., Pöhlker, M. L., Pozzer, A., Schumann, U., Tomsche, L., Williams, J., Zahn, A., Andreae, M., Borrmann, S., Bräuer, T., Dörich, R., Dörnbrack, A., Edtbauer, A., Ernle, L., Fischer, H., Giez, A., Granzin, M., Grewe, V., Harder, H., Heinritzi, M., Holanda, B. A., Jöckel, P., Kaiser, K., Krüger, O. O., Lucke, J., Marsing, A., Martin, A., Matthes, S., Pöhlker, C., Pöschl, U., Reifenberg, S., Ringsdorf, A., Scheibe, M., Tadic, I., Zauner-Wieczorek, M., Henke, R., and Rapp, M.: Cleaner Skies during the COVID-19 Lockdown, Bulletin of the American Meteorological Society, 103, E1796 – E1827, https://doi.org/10.1175/BAMS-D-21-0012.1, 2022.

Voigt, C., Märkl, R., Sauer, D., Dischl, R., Renard, C., Seeliger, K., Yu, F., Kaufmann, S., Bräuer, T., Jurkat-Witschas, T., Le Chenadec, G., Moreau, J., Requena-Esteban, E., Bonne, N., Vals, M., Roche, A., Zelina, J., Dörnbrack, A., Eirenschmalz, L., Heckl, C., Horst, E., Lichtenstern, M., Marsing, A., Neumann, G., Roiger, A., Scheibe, M., Stock, P., Giez, A., Eckel, G., and Le Clercq, P.: Substantial aircraft contrail formation at low soot emission levels, Nature, 652, 112–118, https://doi.org/10.1038/s41586-026-10286-0, 2026.

von Bonhorst, G., Maizet, M., and Gierens, K.: On contrail prediction under realistic weather forecast uncertainty using the example of WAWFOR data, Meteorologische Zeitschrift, https://doi.org/10.1127/metz/1251, 2025.

Wang, Z. and Voigt, C.: Tracing contrails within cirrus clouds and their climate effect, Nature Communications, 16, 10 702, https://doi.org/10.1038/s41467-025-66724-6, 2025.

Wang, Z., Bugliaro, L., Gierens, K., Hegglin, M. I., Rohs, S., Petzold, A., Kaufmann, S., and Voigt, C.: Machine learning for improvement of upper-tropospheric relative humidity in ERA5 weather model data, Atmospheric Chemistry and Physics, 25, 2845–2861, https://doi.org/10.5194/acp-25-2845-2025, 2025.

Widmaier, K., Piontek, D., Kirschler, S., and Voigt, C.: Uncertainties in the prediction of contrail-sensitive airspaces with CoCiP related to meteorological input, aircraft type and heading, Atmospheric Environment: X, ?, ?, https://doi.org/?, 2026.

Wolf, K., Bellouin, N., and Boucher, O.: Sensitivity of cirrus and contrail radiative effect on cloud microphysical and environmental parameters, Atmospheric Chemistry and Physics, 23, 14 003–14 037, https://doi.org/10.5194/acp-23-14003-2023, 2023.

Wolf, K., Bellouin, N., and Boucher, O.: Distribution and morphology of non-persistent contrail and persistent contrail formation areas in ERA5, Atmospheric Chemistry and Physics, 24, 5009–5024, https://doi.org/10.5194/acp-24-5009-2024, 2024.

Wolf, K., Bellouin, N., Boucher, O., Rohs, S., and Li, Y.: Correction of ERA5 temperature and relative humidity biases by bivariate quantile mapping for contrail formation analysis, Atmospheric Chemistry and Physics, 25, 157–181, https://doi.org/10.5194/acp-25-157-2025, 2025.

Yin, F., Grewe, V., Castino, F., Rao, P., Matthes, S., Dahlmann, K., Dietmüller, S., Frömming, C., Yamashita, H., Peter, P., Klingaman, E., Shine, K. P., Lührs, B., and Linke, F.: Predicting the climate impact of aviation for en-route emissions: the algorithmic climate change function submodel ACCF 1.0 of EMAC 2.53, Geoscientific Model Development, 16, 3313–3334, https://doi.org/10.5194/gmd-16-3313-2023, 2023.

https://doi.org/10.5194/jecats-2026-14
Preprint. Discussion started: 14 August 2026

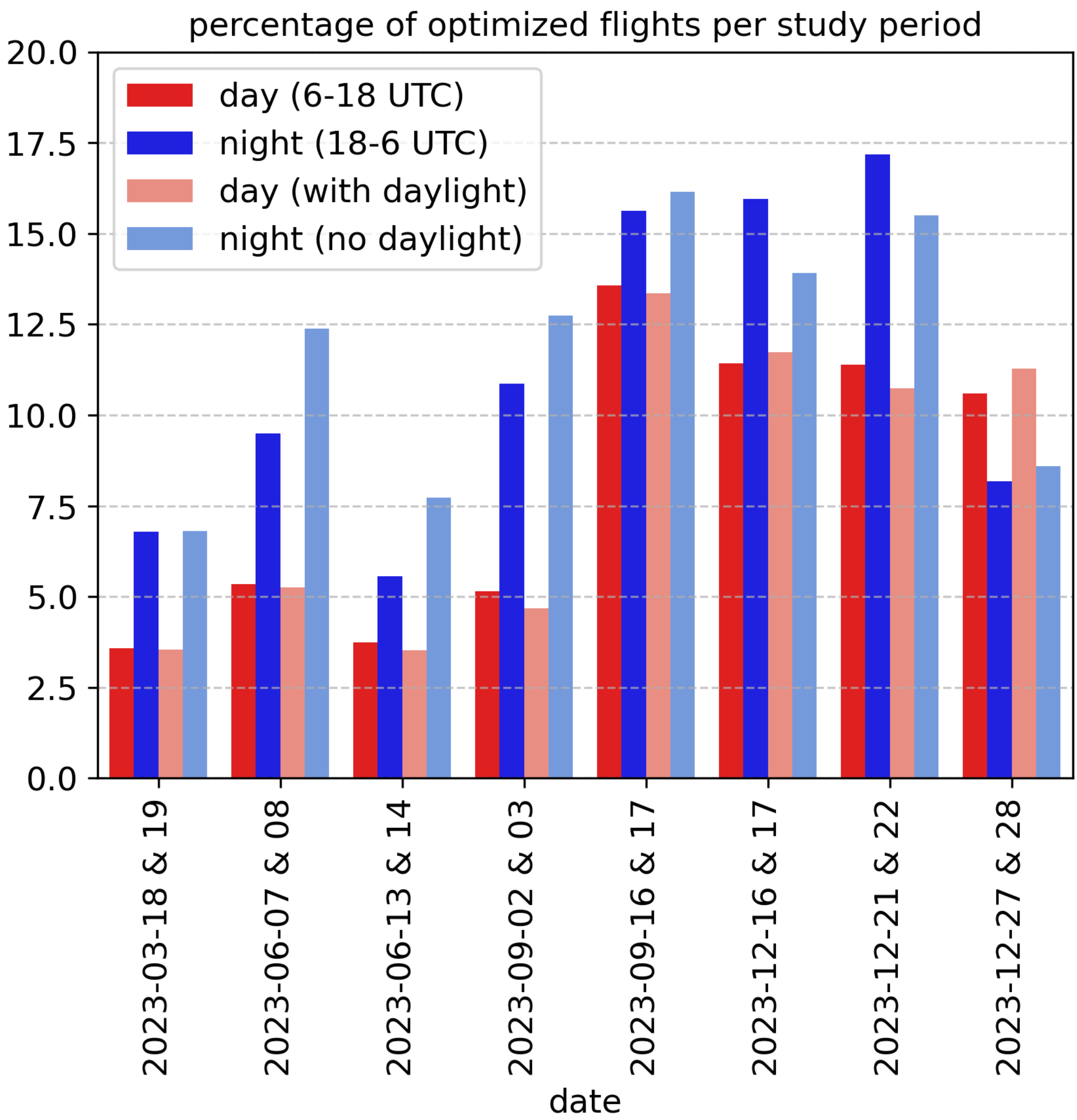

Figure 9. Histogram for the fraction of flights optimized at different times when considering the full optimization. Each flight is evaluated based on its mean time and position. Classes include a static day- and nighttime definition (6–18 UTC and 18–6 UTC, respectively) as well as a solar insolation-dependent definition (considering local sunrise and sunset time).

https://doi.org/10.5194/jecats-2026-14
Preprint. Discussion started: 14 August 2026

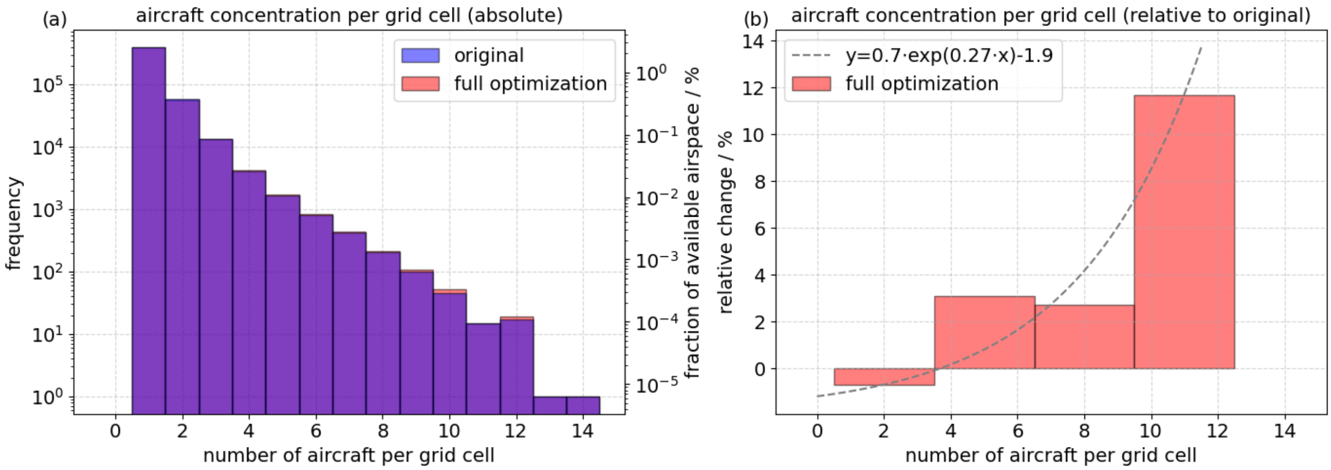

Figure 10. Histogram for a) the distribution of numbers of aircraft per grid cell for the original air traffic (blue) and the fully optimized traffic (red), and b) the relative change between both, including an example expontial function to demonstrate the apparent functional behavior. A grid of 2° × 2° × 1000 ft × 10 min is considered (see text for details).

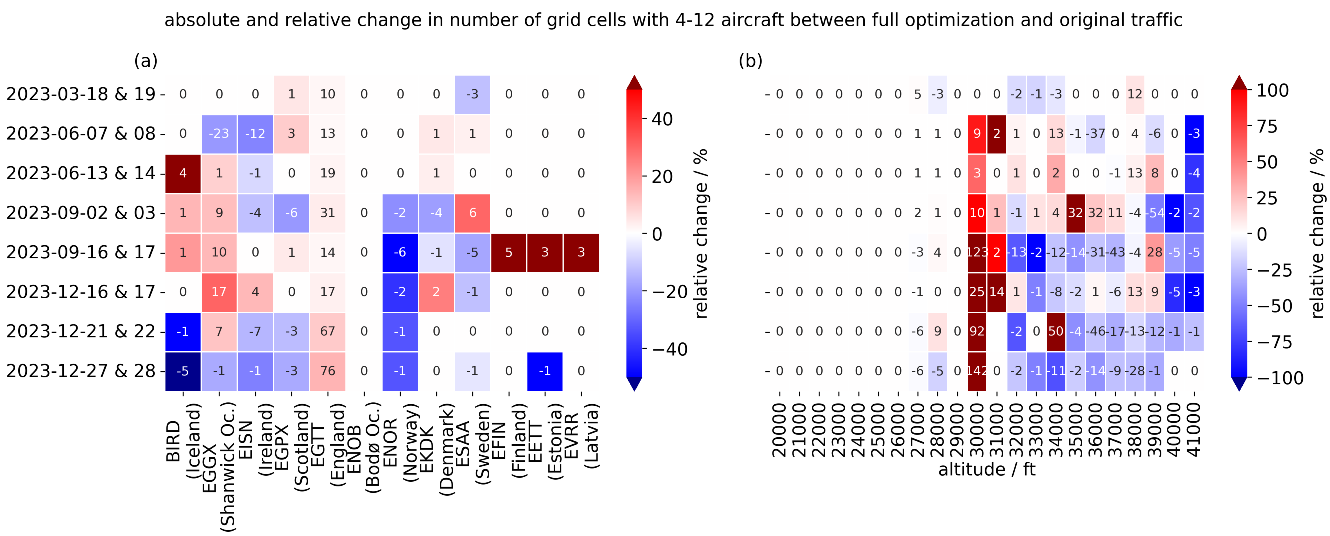

Figure 11. Same data as in Fig. 10 but only cases with 4–12 aircraft per grid cell and visualized against date, and a) ANSP sector or b) altitude. Absolute changes are denoted in the grid cells whereas relative changes are indicated by the color scheme.

https://doi.org/10.5194/jecats-2026-14
Preprint. Discussion started: 14 August 2026

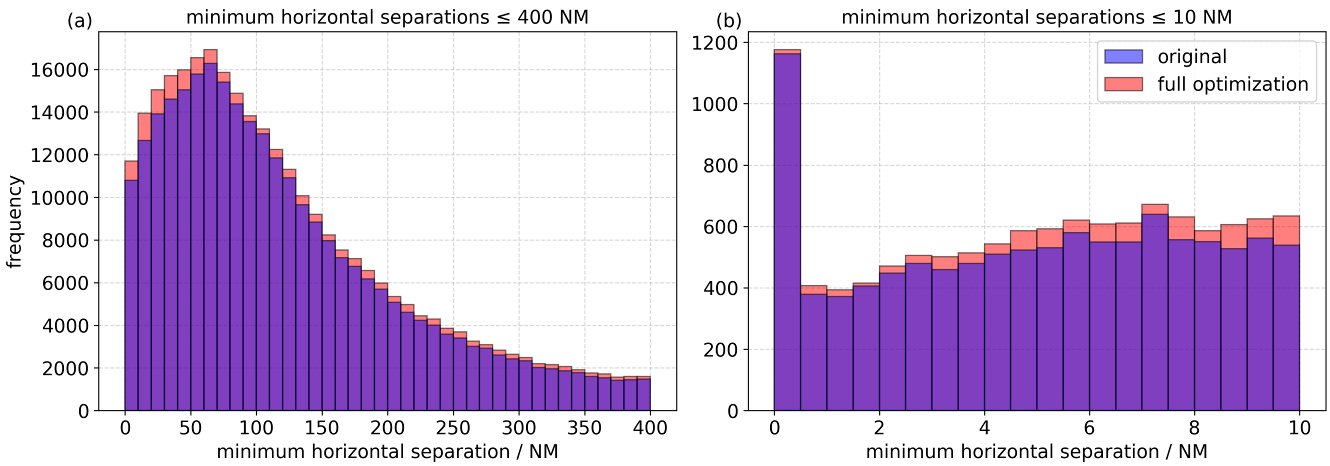

Figure 12. Histograms of the minimal horizontal separation of aircraft pairs for separations up to a) 400 NM (ca. 741 km) and b) 10 NM (ca. 19 km). Separations are given based on the original flight traffic (blue) and the fully optimized traffic (red).

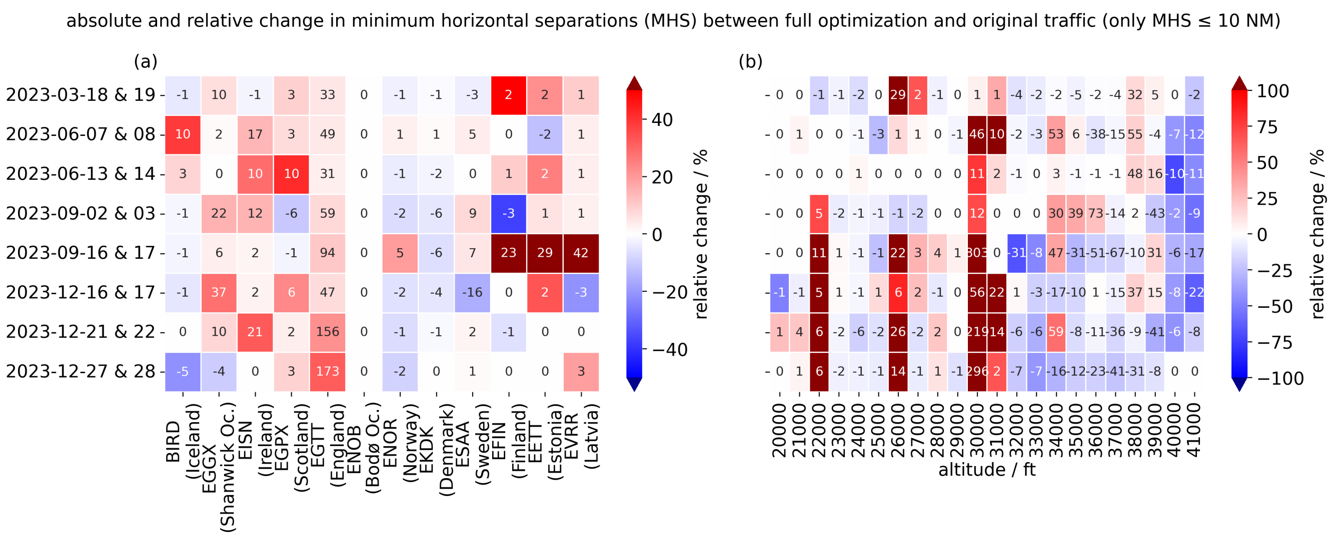

Figure 13. Same data as in Fig. 12 but only cases with a minimum horizontal separation ≤ 10 NM and visualized against date, and a) ANSP sector or b) altitude. Absolute changes are denoted in the grid cells whereas relative changes are indicated by the color scheme.

https://doi.org/10.5194/jecats-2026-14
Preprint. Discussion started: 14 August 2026

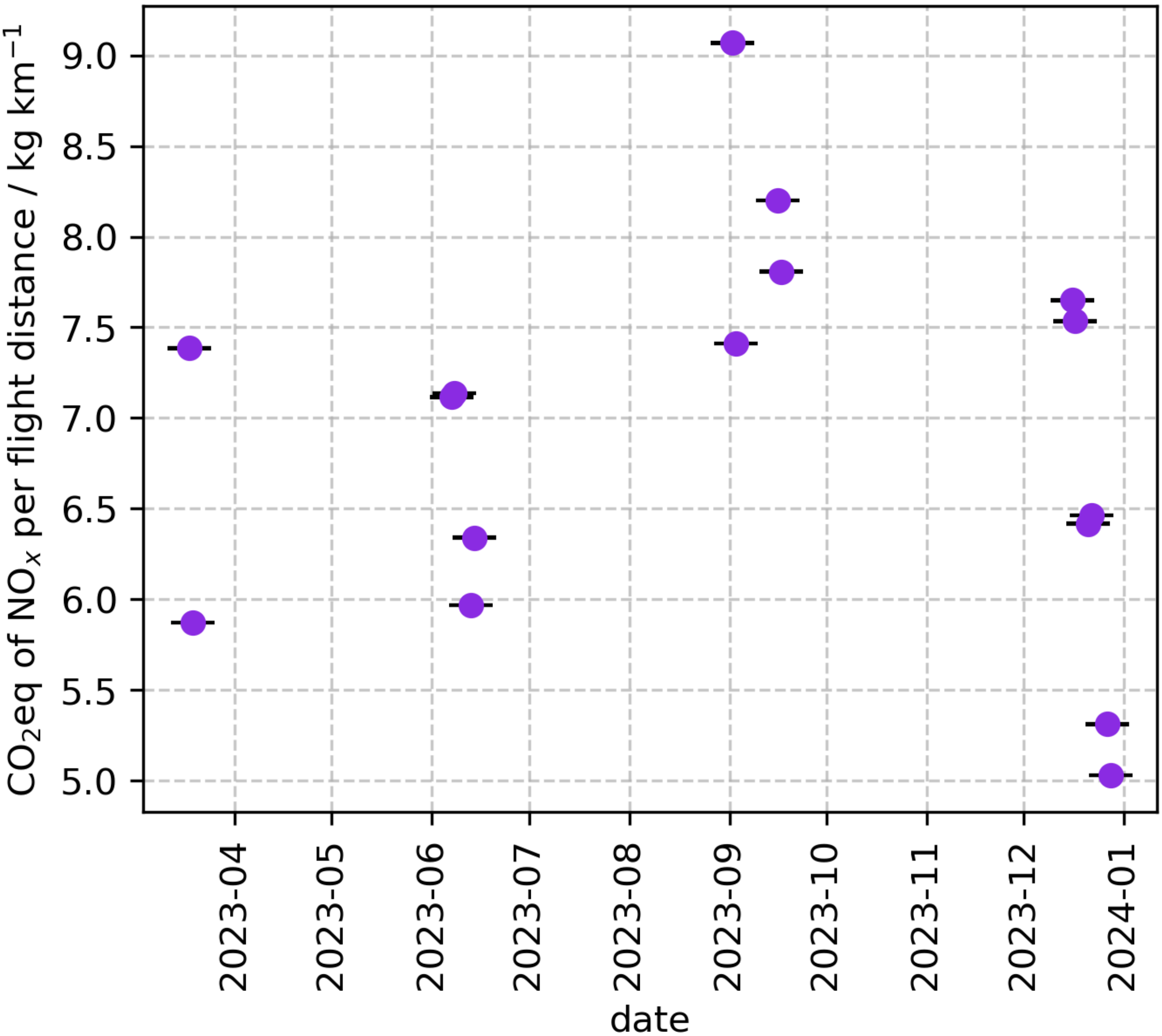

Figure D1. 10-member ensemble mean NO_x emissions per fuel burned for each of the 16 study days from all waypoints within the Borealis alliance airspace for the original air traffic. The uncertainty range indicates the 95 % confidence interval of the mean for the 10-member meteorology ensemble.